

## SELECTIVITY CONTROL UTILIZING ACTIVATION ENERGY DIFFERENCES HYDROGENATION OF CO

N. A. Bhore, K. B. Bischoff, W. H. Manogue, and G. A. Mills  
Center for Catalytic Science and Technology  
Department of Chemical Engineering  
University of Delaware  
Newark, DE 19716

### INTRODUCTION

Multifunctional catalysts offer important opportunities for scientific advances and industrial applications since they are able to activate different molecular species simultaneously. Of critical interest is the molecular structures of the catalyst responsible for such multiple activations, how the activated species interact, and how the reaction dynamics control activity and selectivity.

Hydrogenation of carbon monoxide is a widely studied reaction with many practical applications. The catalytic performances of supported Rh catalysts for CO hydrogenation are very dependent on the support and added modifiers (1-11). Of particular interest is the novel Rh-Mo/Al<sub>2</sub>O<sub>3</sub> catalyst system which displays exceptionally high activity for CO hydrogenation and high selectivity for formation of oxygenates.

Kinetic and characterization tests were carried out using catalysts consisting of Rh on Al<sub>2</sub>O<sub>3</sub> and on TiO<sub>2</sub> with various amounts of added molybdena. The results are discussed in terms of selectivity enhancement by utilizing differences in activation energies for selective and non-selective reactions. Reaction mechanisms are discussed in terms of a dual-site functionality with implications for design of improved catalysts.

### EXPERIMENTAL

Catalysts of composition shown in Table 1 were prepared by impregnation. All contain a nominal 3% Rh from rhodium nitrate solution. The alumina was Catapal and the titania Degussa P-25. Those containing molybdena were prepared in stages. The support was first impregnated with ammonium molybdate, pH 1, followed by drying and air calcination. Then rhodium was deposited. For the 15% Mo catalysts, a dual impregnation was used to overcome solubility limitation. Before testing, catalysts were reduced in flowing H<sub>2</sub> at 500° [All temperatures are °C]. Performance testing was in a flow reactor system. Data were obtained at 3 MPa, H<sub>2</sub>/CO = 2, at 3000 to 36,000 GHSV, 200° to 250°. Steady state product analysis was by on-line GC. To make comparisons, space rates were varied at constant temperature to obtain equal conversions (limited to 6%), then conversions were "normalized" to 3000 GHSV by multiplying by the factor : actual GHSV/3000. The reaction has been shown not to be mass or heat transfer limited (8). CO and irreversible H<sub>2</sub> chemisorption were measured at room temperature, the former using a pulse injection system and a thermal conductivity detector, and the latter using a static system. Previous to measurements, catalysts were reduced under the same schedule as for reactor runs.

### RESULTS AND DISCUSSION

Catalyst composition — effect on performance. The activity of supported Rh catalysts for CO hydrogenation at 250° was found to be TiO<sub>2</sub>-500 > TiO<sub>2</sub>-300 > Al<sub>2</sub>O<sub>3</sub> > SiO<sub>2</sub>. For TiO<sub>2</sub>, 500 and 300 refers to the reduction temperature used before testing. Detailed data for Rh/TiO<sub>2</sub> and Rh/Al<sub>2</sub>O<sub>3</sub> are found in Table 1. The effect of modifiers was also studied, particularly for selectivity enhancement. In this paper, selectivity refers to the conversion of CO to oxygenates relative to hydrocarbons. The results of some of the various modifiers on the selectivity of Rh/Al<sub>2</sub>O<sub>3</sub> and of Rh/TiO<sub>2</sub> are shown in Fig. 1. The line which is drawn for Rh/Al<sub>2</sub>O<sub>3</sub>, shows that selectivity decreases moderately with increasing conversion. The Mo-modified catalysts are unique in their high activities and increased selectivities (4,6,7,8,9). For instance the activity was increased 12-fold by addition of 7.5% Mo. A 4% conversion was obtained at 225° at 18,000 GHSV, and selectivity was 73%. When measured at 250°C, the % selectivity increased progressively with added % Mo : 29-0; 58-2.8; 65-7.5; 69-15, Table 1.

Molybdena added to Rh/TiO<sub>2</sub> was also effective in increasing activity and selectivity, Table 1.

In addition, molybdena brought a high capability for the shift-conversion reaction with as much as 25% of the converted CO going to CO<sub>2</sub>. The amount of CO<sub>2</sub> observed is consistent with the reaction  $\text{CO} + \text{H}_2\text{O} \longrightarrow \text{CO}_2 + \text{H}_2$  utilizing the amount of water produced from formation of hydrocarbons and higher alcohols.

Temperature — effect on catalyst performance. The rates of formation of some of the products as a function of temperature have been published previously (6) and additional data are shown in Fig. 2. The calculated values of apparent  $E_{\text{act}}$  given in Table 2 for overall CO conversion is the same for Rh/Al<sub>2</sub>O<sub>3</sub> and Rh/MO/Al<sub>2</sub>O<sub>3</sub>. Hence higher reaction rates with the latter catalyst is not due to a lower  $E_{\text{act}}$ . It should also be noted that for the Rh-Mo/Al<sub>2</sub>O<sub>3</sub> catalysts  $E_{\text{act}}$  for oxygenates as a group is 18.6 Kcal/mole, much lower than the 31.2 volume for hydrocarbons. Individual products show smaller but significant differences from these values, for example 32.4 for CH<sub>4</sub> and 27 for C<sub>2</sub>H<sub>6</sub>. The consequence is that there is a double penalty for operation at higher temperatures. Not only are hydrocarbons increased relative to oxygenates, but also the hydrocarbons consist of larger amounts of less valuable CH<sub>4</sub>. It is also significant that  $E_{\text{act}}$ , C<sub>2</sub>+oxy. >  $E_{\text{act}}$ , C<sub>1</sub>oxy. This is believed due to the circumstance that CO dissociation is required for hydrocarbons and higher alcohols but not C<sub>1</sub> oxygenates.

Utilizing activation energy differences for selectivity control. The wide differences in  $E_{\text{act}}$  between formation of oxygenates and hydrocarbons results in a more rapid decrease in the rate of formation of hydrocarbon relative to oxygenates as temperature is decreased. Selectivity is increased. The relative rates for selective,  $r_o$ , and non-selective,  $r_h$ , reactions are expressed by the relationship

$$\frac{r_o}{r_h} = \frac{\text{selectivity to oxygenates}}{\text{selectivity to hydrocarbons}} = D \cdot e^{\frac{-(E_o - E_h)}{RT}}$$

D is a constant whose value,  $\log D = -5.60$ , was established from experimental selectivities for Rh/7.5Mo/Al<sub>2</sub>O<sub>3</sub>. The following selectivities to oxygenates represent those calculated and found and those predicted for various temperatures.

Temp.°	273	250	225	200	180	160	140
Calculated %	50	61	75	85	91	95	98
Found %		65	73	86			

One application of this calculation is to provide a prediction of the selectivities which may be obtained with catalysts of sufficient activity to be used at lower temperatures.

The use of lower temperatures to increase selectivity has a penalty — namely loss of conversion rate. The decrease in rate can also be calculated for selective and nonselective reactions as a function of temperatures:

$$\frac{\text{rate } T_1}{\text{rate } T_2} = e^{\frac{-E(T_1 - T_2)}{RT_1 T_2}}$$

This is illustrated by the following:

	oxygenates	hydrocarbon
$E_{\text{act}}$ cal/mole	18,600	31,200
50° decrease, 250° - 200°	7 fold	24 fold
90° decrease, 250° - 160°	42 fold	524 fold

The above calculations can provide the initial basis for optimizing process design in which advantages of increased selectivity — improved product value, lower plant and operations costs for separation, and possible longer catalyst life — are calculated and related to disadvantages of lower rates of conversion — larger catalyst inventory and increased reactor investment. Thus an increase of selectivity from 65 to 86% for Rh/7.5%Mo/Al<sub>2</sub>O<sub>3</sub> in going from 250° to 200° may more than compensate for the requirements imposed by a 7-fold increase in catalyst inventory to reach the same conversion level.

Rate comparisons with other catalysts. It is of interest to compare the space-time-yield for Rh/Mo/Al<sub>2</sub>O<sub>3</sub> catalyst and industrial Cu/ZnO/Al<sub>2</sub>O<sub>3</sub> catalysts. The STY for Rh/7.5%Mo/Al<sub>2</sub>O<sub>3</sub> at 250° at 36,000 GHSV in g/hr/ml catalyst corresponds to 1.0 for all products, 0.76 for oxygenates and hydrocarbons, or 0.4 for oxygenate liquids (0.51 ml/hr/g). Commercial catalysts are said to produce 0.5 ml methanol/hr/ml cat. Thus the Rh/Mo/Al<sub>2</sub>O<sub>3</sub> catalyst is as active as commercial catalyst. They are by far the most active of supported Rh catalysts identified in a wide survey (11).

Kinetics. The coefficients of the kinetic power-law rate expression for CO hydrogenation

$$\text{Rate}_{\text{species}} = A \cdot p_{\text{H}_2}^x \cdot p_{\text{CO}}^y$$

were determined for Rh/Al<sub>2</sub>O<sub>3</sub> and Rh/Mo/Al<sub>2</sub>O<sub>3</sub>, Table 3 (3,6,8). A negative value for the exponent of pCO for the Rh/Al<sub>2</sub>O<sub>3</sub> catalysts is interpreted to indicate that there is an inhibition of the reaction by preferential adsorption of CO relative to H<sub>2</sub> on the Rh. However, for the Mo-modified catalyst the exponent of pCO is zero for the overall conversion of CO, for MeOH and for CO<sub>2</sub> formation. While CO<sub>2</sub> is mechanistically a secondary product, it follows the power-law because product water is immediately converted to CO<sub>2</sub>. Significantly, the exponent of pCO remains negative for the formation of methane and higher alcohols. This is interpreted to mean that formation of CH<sub>4</sub> and higher alcohols is occurring at Rh sites, and that dissociation of CO is involved which is subject to inhibition by CO. Formation of methanol does not involve CO dissociation and is not inhibited by CO.

H<sub>2</sub> and CO chemisorption and turnover frequency. The dispersion of Rh in the Rh/Al<sub>2</sub>O<sub>3</sub> catalyst was determined to be 39%, based on H<sub>2</sub> chemisorption and assuming 1H/1Rh. However, for Mo catalysts, H<sub>2</sub> cannot be used for this purpose because of the formation of non-stoichiometric Mo bronzes. Therefore, CO was used to measure Rh dispersion for Mo catalysts. H<sub>2</sub> adsorption on Rh/Al<sub>2</sub>O<sub>3</sub> provided an initial calibration point. It was determined that CO does not adsorb appreciably on partially reduced molybdena under the above-mentioned conditions. While CO can adsorb in different forms, as determined by infrared measurements, it is assumed that the stoichiometry of CO chemisorption on Rh does not change with increased Mo and can be used as a measure of Rh dispersion. The amount of CO chemisorbed decreased progressively and substantially with addition of molybdena, Table 4. Also shown is the overall rate of CO conversion, labelled the turn-over-frequency, for each Rh atom in the sample. The TOF shows an increase as increasing amounts of Mo are added. Thus, even though the number of CO adsorption sites decreases, the rate of CO conversion increases. Furthermore, more impressive increases are observed if the comparison is done on the TOF based on each CO adsorption site. Thus at 15% Mo, the overall activity per CO site increased by 150 fold!

## CONCLUSIONS AND COMMENTS

The exponential form of the reaction rate dependence on activation energy and temperature makes rates very sensitive to activation energies and temperatures. As a consequence, differences in activation energies between selective and non-selective reactions can provide for significantly increased selectivities at lower temperatures. Decreasing reaction temperatures from 250° to 200°, for Rh-MoAl<sub>2</sub>O<sub>3</sub> for example, increases selectivity to oxygenates (E<sub>act</sub> 18.6 Kcal/mole) from 65% to 85% relative to hydrocarbons (E<sub>act</sub> 31.2 Kcal/mole). Reaction rates are decreased 7-fold. The selectivity is predicted to increase to 98% at 160°. Changes in the distribution of individual hydrocarbons and oxygenates with reaction temperature are also predicted. Such considerations provide a preliminary basis for process optimization through temperature selection.

The greatly enhanced activity and selectivity imparted by Mo addition to Rh/Al<sub>2</sub>O<sub>3</sub> is not explained by activation energy differences alone. Gilhooy, Jackson and Rigby (5) found wide variations in the apparent activation energies and pre-exponential factors for Rh on various supports. They concluded that the compensation effect, which involves the pre-exponential factor, made conclusions on mechanism ambiguous.

Examination of the power-law exponents presented here show that the rate of hydrogenation of CO to hydrocarbons and oxygenate is inhibited by CO over Rh/Al<sub>2</sub>O<sub>3</sub> but not for methanol formation over Rh-Mo/Al<sub>2</sub>O<sub>3</sub>. Interestingly, the inhibition for CH<sub>4</sub> formation remains. The implication is that the mechanism of the rate determining step for methanol differs from methane and that the latter is dependent on the Rh.

Based on these results and other characterization tests (8), it is proposed that Rh-Mo/Al<sub>2</sub>O<sub>3</sub> catalysts operates by a dual site mechanism in which CO is activated by Rh and hydrogen is activated by MoO<sub>(3-x)</sub> with migration of activated hydrogen to the activated CO. A major point is that while Rh is capable of activating H<sub>2</sub>, its activation is inhibited by CO during CO hydrogenation. In contrast, H<sub>2</sub> activation by MoO<sub>3-x</sub> is not inhibited by CO. As a consequence of increasing the hydrogenation capability, which is rate-limiting, the overall catalytic activity for CO conversion is greatly accelerated. The increase in oxygenates is also due to increased hydrogenation ability which shows up particularly in methanol formation. The formation of hydrocarbons and higher alcohols involve CO dissociation believed to occur on Rh. As the power-law data show, their formation even over Rh-Mo/Al<sub>2</sub>O<sub>3</sub> is inhibited by CO which is visualized as strongly occupying the Rh sites.

For the practical purpose of achieving higher selectivities at lower temperatures, say 160°, catalysts of increased activity are required. The results discussed here are believed to provide a guide for design of improved dual-site catalysts. The search should be for a structure which provides a H<sub>2</sub> activation site not inhibited by CO. It is speculated that to fulfill this role requires a non-metallic, non-stoichiometric structure such as a partially reduced oxide. For Mo catalysts there is the potential for improvements by use of unusual oxide structures, or of reduction to a MoO<sub>3-x</sub> of more optimum level, or possibly by use of sulfides instead of oxides. A better knowledge of the interface of Rh and partially reduced molybdena is of great interest as well as the mobility of activated hydrogen to or from the Rh (4,8). The extremely high increase in activity, namely 150-fold, of Rh sites identified by CO chemisorption on the 15% Mo/Rh/Al<sub>2</sub>O<sub>3</sub> catalyst, illustrates the possibility of catalysts with greatly increased activity. These could be used with great advantage at lower temperatures than present industrial catalyst.

#### ACKNOWLEDGEMENTS

Early experimental and conceptual contributions by Dr. C. Sudhakar are recognized. This work was supported by the Department of Energy Grant DE-FG22-84PC70780.

#### REFERENCES

1. Wilson, T.P., Kasai, P.M., Ellgen, P.C. *J. Catal.* **69**, 193-201 (1981).
2. van den Berg, F.G.A., Glezer, J.H.E., Sachtler, W.M.H. *J. Catal.* **93**, 340-352 (1985).
3. Underwood, R.P., Bell, A.T. *Applied Catal.* **21**, 157 (1986).
4. Jackson, S.D., Braneth, B. J., Winstanley, D. *Applied Catal.* **27**, 325-333 (1986).
5. Gilhooy, K., Jackson, S.D., Rigby, S. *Applied Catal.* **21**, 349 (1986).
6. Sudhakar, C., Bhole, N.A., Bischoff, K.B., Manogue, W.H., Mills, G.A. in *Catalysis 1987*, Ward J.W., Ed., Elsevier Sc. Pub. Amsterdam, 115-124 (1988).
7. Bhole, N.A., Sudakar, C., Bischoff, K.B., Manogue, W.H., Mills, G.A. in *Catalysis: Theory to Practice*, Phillips, M. J., Tiernan, M., Eds., Chem. Inst. Canada, Ottawa v. 2 594-601 (1988) v5 (1989).
8. Bhole, N.A. *Modifiers in Rhodium Catalysts for Carbon Monoxide Hydrogenation: Structure - Activity Relationships*. Ph.D. Thesis, University of Delaware, 1989.
9. Kip, J. B., Hermans, E.G.F., Van Wolput, J.M.H.C., Hermans, N.M.A., van Grondelle, J., Prins, R. *Applied Catal.* **35**, 109-139 (1987).

10. Arakawa, H., Hamaoka, T., Takeuchi, K., Matsuzaki, T., Sugi, Y. ref. 6, v 2, 602-609 (1988).  
 11. Klier, K. in *Coal Liquefaction — A Research & Development Needs Assessment*. DOE Contract DE-AC01-87ER30110 (1989).

Table 1. CO Hydrogenation by Catalysts of Various Compositions, H<sub>2</sub>/CO=2; 3MPa.  
 All contain 3% Rh.

	0% MoAl <sub>2</sub> O <sub>3</sub>		2.8% Mo Al <sub>2</sub> O <sub>3</sub>	7.5% Mo Al <sub>2</sub> O <sub>3</sub>				15% MoAl <sub>2</sub> O <sub>3</sub>		6% Mo TiO <sub>2</sub>	
	250 3000	275 3000	225 3000	200 3000	225 18000	235 18000	250 36000	200 3000	225 3000	225 4700	250 11230
% Conversion of CO, includes CO <sub>2</sub>											
Conv. to CO <sub>2</sub>	5.7 1	12.5 1	9.0 21.5	7.3 23.9	4.0 23.0	6.0 25.6	5.3 24.5	6.0 25	27 37	11.2 35	12.3 38
% of CO Converted, excludes CO <sub>2</sub>											
CH <sub>4</sub>	60	69	34.8	9.4	18.4	23.8	26.8	7.2	10.6	27.4	35
C <sub>2</sub> H <sub>6</sub>	4	4.1	4.5	3.1	5.8	4.7	5.9	2.4	4.4	11.6	15.3
C <sub>3</sub> H <sub>8</sub>	5	5.0	1.5	1.1	2.3	1.9	2.3	0.9	1.6	4.7	5.5
C <sub>4</sub> H <sub>10</sub>	2	1.4	0.4	0.3	0.6	0.5	0.6	0	0.5	1.6	2
C <sub>5</sub> H <sub>12</sub>		2.0		0	0	0	0			0	0
Total HCs	71	81.5	41.7	13.9	27.1	30.9	35.6	10.5	17.1		
MeOH	2	0.8	13.4	37.6	21.7	17.7	15.7	24.0	10.9	38.9	26
MeOMe	1	0.2	15.9	30.0	28.3	26.9	26.5	39.5	56.5	3.1	4.5
MeCHO	2	2.3	0	0	0	0	0	0	0	0	0
EtOH	11	5.2	12.3	5.8	7.4	7.4	6.7	18.0	1?	7.5	6.4
MeOAc	3	2.6	2.4	1.1	1.1	0.7	0.7	0.2	0.7	2.1	1.7
HOAc	0	0	0	0	0	0	0	0	0	0	0
EtCHO	0.4	0	0	0	0	0	0	0	0	0	0
C <sub>3</sub> H <sub>7</sub> OH	2.7	2.5	2.4	1.9	0.9	2.2	0.7	2.4	2.7	1.4	1.2
MeOEt	3	21.	12.6	9.9	14.0	14.5	14.5	7.0	11.2	3.0	2.5
EtOAc	3	3.6	0	0	0	0	0	0	0	0	0
C <sub>4</sub> H <sub>9</sub> OH	0	0.6	0	0	0	0	0	0	0.4	0	0
Total Oxy.	28.9	18.9	58.7	86.3	73.3	69.2	64.8	90	83	56	39
C <sub>1oxy.</sub>	5.1	2.6	34.3	71.4	55.0	49.6	47.3	65.9	71.3	43.6	30.8
C <sub>2oxy.</sub>	20.7	14.2	22.2	13.0	17.4	17.4	16.8	22.8	8.9	10.9	8.6
C <sub>3oxy.</sub>	3.0	2.5	2.4	1.9	0.9	2.2	0.7	2.4	2.6	1.4	1.2
C <sub>2+oxy.</sub>											
% of oxy.	82.4	86.2	41.6	17.2	21.7	28.1	26.7	27.7	14.0	19	21

Table 2. Apparent Activation Energies, CO Hydrogenation

	Product	Kcal/g mol
3% Rh/Al <sub>2</sub> O <sub>3</sub> 3% Rh/7.5% Mo/Al <sub>2</sub> O <sub>3</sub>	-CO	21.3 ± 0.3
	-CO	21.6 ± 0.9
	C <sub>1oxy</sub>	17.2 ± 0.7
	C <sub>2oxy</sub>	24.3 ± 2.4
	<u>C<sub>total oxy</sub></u>	<u>18.6 ± 0.9</u>
	CH <sub>4</sub>	32.3 ± 2.6
	C <sub>2</sub> H <sub>6</sub>	27.5 ± 3.6
	C <sub>3</sub> H <sub>8</sub>	28.6 ± 4.1
	C <sub>4</sub> H <sub>10</sub>	26.3 ± 2.9
	<u>C<sub>total HC</sub></u>	<u>31.2 ± 2.5</u>
	CO <sub>2</sub>	21.9 ± 0.7

Table 3. Power Law Coefficients for CO Hydrogenation Rates<sub>species</sub> = A · P<sub>H<sub>2</sub></sub><sup>x</sup> · P<sub>CO</sub><sup>y</sup>

Catalyst	Species	x	y
3%Rh/Al <sub>2</sub> O <sub>3</sub> 3%Rh-15%Mo/Al <sub>2</sub> O <sub>3</sub>	-CO	0.8	-0.3
	-CO	0.72 ± 0.05	-0.03 ± 0.09
	+CH <sub>4</sub>	1.02 ± 0.08	-0.32 ± 0.09
	+CH <sub>3</sub> OH	1.53 ± 0.01	-0.01 ± 0.11
	+C <sub>2+oxy</sub> .	0.91 ± 0.23	-0.47 ± 0.23
	+CO <sub>2</sub>	0.38 ± 0.05	-0.04 ± 0.06

Table 4. CO Chemisorption and Site Reactivity (TOF) as Function of Mo in 3%Rh,x%Mo/Al<sub>2</sub>O<sub>3</sub>.

Wt% Mo	CO Chemisorption μ moles/g	% Dispersion of Rh	#CO Reacted/site-sec.**	
			per atom Rh	per site Rh***
0	112	39*	0.4	1
2.8	74	26	4.0	15
7.5	46	16	8.0	50
15.0	28	10	15.0	150

\* Determined by H<sub>2</sub> chemisorption.

\*\* CO Hydrogenation at 225°.

\*\*\* Per CO site.

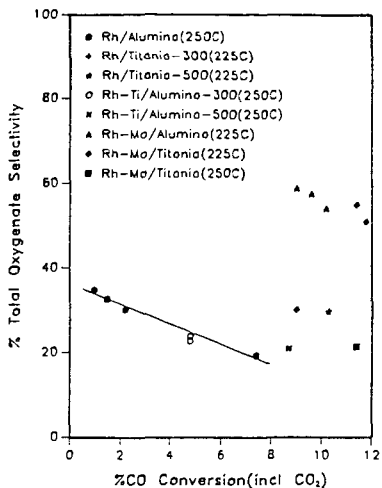


Figure 1. Effect of Catalyst Composition and Conversion Level on Selectivity to Oxygenates. 3%Rh on  $\text{Al}_2\text{O}_3$  or on  $\text{TiO}_2$  Modified by 1 Atom Mo or Ti per Atom Rh. CO Hydrogenation 3MPa,  $\text{H}_2/\text{CO}=1$ , Various Space Rates (Run Temp. °C).

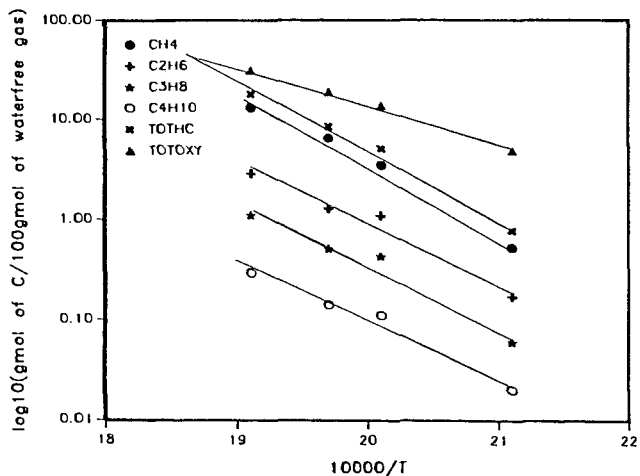


Figure 2. Rates of Formation of Hydrocarbons and Total Oxygenates Over 3%Rh/7.5%Mo/ $\text{Al}_2\text{O}_3$ . 3MPa  $\text{H}_2/\text{CO}=1$ . Rates Normalized to 3000 GHSV. See Table 2 for  $E_{\text{act}}$ .

## DEHYDROCOUPLING OF METHANE BY SUPPORTED ORGANOMETALLIC COMPLEXES

Robert B. Wilson Jr., Yee-Wai Chan, and Barry M. Posin  
Inorganic and Organometallic Chemistry Program  
SRI International, Menlo Park, CA, 94025

### INTRODUCTION

Two possibilities exist for dehydrocoupling of methane to higher hydrocarbons: The first is oxidative coupling to ethane/ethylene and water that is the subject of intense current research interest. As Labinger<sup>1</sup> and others have recently pointed out, oxidative coupling has an apparent upper limit on yield of C<sub>2</sub> hydrocarbons of around 30% at atmospheric pressure. Non-oxidative coupling to higher hydrocarbons and hydrogen is endothermic, but in the absence of coke formation the thermodynamic yield of hydrocarbons varies between 25% at 827 °C and 65% at 1100 °C and atmospheric pressure.<sup>2</sup> Additionally, after separation the unreacted methane can be recycled unlike oxidative coupling. These numbers are very attractive and a number of recent reports have appeared that prove this concept.<sup>3-9</sup> Yamaguchi's results are particularly interesting because he reported ~ 50% conversion of methane and ~ 85% selectivity to "aromatic oil" at 1300 °C. These values are very close to the thermodynamic equilibrium values.

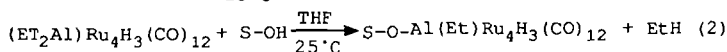
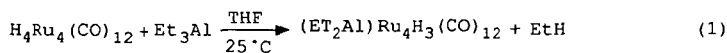
### RESULTS AND DISCUSSION

Research on the technique of surface confinement to produce novel catalysts for a wide variety of processes is continuing in many laboratories.<sup>10-13</sup> We have been working on the development of novel surface confined catalysts to dehydrocouple methane. The catalysts are prepared by reacting organometallic complexes of transition metals with inorganic oxide supports to produce surface-confined metal complexes.<sup>14</sup> The increased activity of highly dispersed catalysts is desirable for activating the relatively inert methane and additionally highly dispersed catalysts are resistant to coking. The use of zeolitic supports will provide further stabilization of the highly dispersed catalysts which are confined inside the zeolite pores. The variables we are studying include cluster size, supporting materials, and reaction conditions.

Synthesis of catalysts- The synthesis of these catalysts involves three steps. The first step is to synthesize the ruthenium cluster precursors. The second step is a novel approach developed in our laboratory involving the reaction of the organometallic clusters with alkyl aluminum. The final step is to anchor these catalysts on supports by a chemical reaction between the hydroxy group of the support and the alkyl groups of the organometallic cluster to give a covalent chemical bond.

The organometallic complexes include: a mono-ruthenium complex, Ru(allyl)<sub>2</sub>(CO)<sub>2</sub>; a tetrameric ruthenium cluster, H<sub>4</sub>Ru<sub>4</sub>(CO)<sub>12</sub>; a hexameric ruthenium cluster, H<sub>2</sub>Ru<sub>6</sub>(CO)<sub>18</sub>; and a mixed metal cluster, H<sub>2</sub>FeRu<sub>3</sub>(CO)<sub>13</sub>. All of these complexes are prepared according to literature procedures.<sup>15,16</sup> The hydrido clusters reacted with triethyl aluminum at room temperature (eq. 1). The reaction stoichiometries

are determined by measuring the quantity of ethane produced.<sup>14</sup> These alkyl aluminum carbonyl ruthenium clusters react with acidic supports:  $\beta$ -alumina, 5A molecular sieves, and LZ-Y 52 zeolite. The reaction stoichiometries are again determined by measuring the quantity of ethane produced (eq. 2).



The monomeric ruthenium complex reacts directly with the acidic support to release one equivalent of propylene. The tetraruthenium and the mixed iron-ruthenium clusters have also been supported on magnesium oxide by the reaction of the acidic hydride and the basic groups on the MgO surface. All supporting materials are in powder form except for the 5A molecular sieves which was 60-80 mesh.

The ruthenium catalysts were tested at 750°C under 150 psig pressure. The results are summarized in Table 1. We used a commercial ruthenium catalyst which is supported on alumina (obtained from Engelhard) for comparison. The metal loadings were based on elemental analyses (Galbraith Laboratory). The flow-rate of input gases (20% methane in helium) were varied due to the detection limit of our GC. Effect of flow-rate will be discussed later.

**Effects of cluster size** - The commercial ruthenium catalyst gives a very high conversion of methane (71.2%) but no hydrocarbon product. Methane conversion on the mono-ruthenium catalysts are considerably lower than the ruthenium clusters ( $\text{Ru}_4$  and  $\text{Ru}_6$ ). In general, methane conversions depend on the type of support and decrease in the order alumina, 5A molecular sieve, and zeolite. These results suggested that the methane conversion is related to the amount of surface bonded metal. On alumina, the metals are located on the surface while on 5A molecular sieves and on zeolite, increasing amounts of metal are located inside the zeolite pore. The  $\text{Ru}_4$  catalysts demonstrated the greatest dependence on the support, the conversion decreased from 10.1 to 4.9 and to 1.7% on alumina, 5A molecular sieve, and Y-zeolite, respectively.

Our intention in using different supports is to confine the ruthenium cluster at different location on or within the support. Hence, the  $\text{Ru}_4$  and  $\text{Ru}_6$  clusters are dispersed on the alumina surface but are confined inside the pores of the zeolite supports. The pore size of the 5A molecular sieve is too small for the  $\text{Ru}_6$  cluster but should be large enough for the  $\text{Ru}_4$  cluster. Since the Y-zeolite has the largest pore (~17Å), most of the  $\text{Ru}_4$  or  $\text{Ru}_6$  clusters are located inside the zeolite pore.

**Product selectivity** - All the ruthenium catalysts produced  $\text{C}_2$  hydrocarbons which included ethane and ethylene. The selectivity of  $\text{C}_2$  hydrocarbon observed with  $\text{Ru}_4$  cluster catalysts increased as the percent conversion of methane decreased. These results also suggest the advantage of having the metal cluster confined inside the zeolite cage. The  $\text{Ru}_6\text{AL}$  has the highest total hydrocarbon yield which is probably due to the higher metal loading. The total hydrocarbon yield for  $\text{Ru}_6\text{MS}$  and  $\text{Ru}_6\text{ZL}$  are about the same, but the  $\text{Ru}_6\text{ZL}$  has a higher selectivity for  $\text{C}_2$  product. Confining the metal cluster inside the zeolite cage may also limited the propagation of methane polymerization. The ruthenium

monomers gave relatively low hydrocarbon yields indicating that polymerization of methane required more than one metal atom.

Coking - The results listed in Table 1 show that more than one equivalent of hydrogen was produced per methane reacted, which suggests coke formation. The elemental analyses listed in Table 2 show that the Ru<sub>4</sub>AL, Ru<sub>4</sub>MS, Ru<sub>6</sub>AL and Ru<sub>6</sub>MS catalysts contained more carbon after reaction with methane. In contrast, the carbon content of Ru<sub>4</sub>ZL decreased after reaction. This phenomena indicates that those catalysts that have metal dispersed on the support surface promote coke formation while the metals confined inside the zeolite cages do not. For Ru<sub>4</sub>MS, the carbon content only increased slightly to 4.38% as compared with more than 20% for the Ru<sub>4</sub>ZL which suggests that a portion of the metal clusters are located inside the cages of the support. The decrease of carbon content on Ru<sub>4</sub>ZL was due to the decomposition of the ruthenium complexes, i.e. release of carbon monoxide.

Effect of reaction conditions - The effect of reaction temperature is similar for every catalyst. Higher methane conversion and product yield are obtained at higher temperatures. Increasing the reaction pressure has a similar effect on the methane conversion. However, the product selectivities for hydrogen and C<sub>2</sub> hydrocarbons decrease but increases for C<sub>6+</sub> hydrocarbons (Table 3). Highest selectivity is observed at 150 psig. As expected, increasing the space velocity lowers the methane conversion but increases the selectivity for hydrocarbon products.

Basic support and mixed metal cluster - Methane conversion over the magnesia supported ruthenium monomer and the FeRu<sub>3</sub> cluster are much higher than the zeolite supported analogs (Table 4). However, the product selectivities to hydrocarbons are lower.

For the mixed iron-ruthenium catalysts, magnesia support also increases the methane conversion. At 600°C, the methane conversion was 8.87% for FeRu<sub>3</sub>MgO and was 3.07% for FeRu<sub>3</sub>ZL. At 750°C, methane conversion increased to 41.5% and 23.05% for FeRu<sub>3</sub>MgO and FeRu<sub>3</sub>ZL, respectively. These catalysts behave similarly to the ruthenium monomers that the hydrocarbon yields were lower on the magnesia supported catalyst.

In-Situ FTIR - In-Situ diffuse reflectance FTIR is being used to study these catalysts. Our diffuse reflectance FTIR (DRIFTS) technique is very similar to the ones recently reported by Vannice<sup>17</sup> and Moser.<sup>18</sup> We have been able to collect data using this system up to 600 °C.

Figure 1 demonstrates the kind of data that can be collected using this FTIR technique. In Figure 1 we have compared the thermal behavior of two of the clusters (FeRu<sub>3</sub> and Ru<sub>4</sub>) supported on MgO under N<sub>2</sub>. The carbonyl stretching region of the spectra is shown starting in the upper left at 25 °C. The two spectra are different as would be expected for the different clusters. The Ru<sub>4</sub> spectra is very similar to that observed by Gates<sup>19</sup> for H<sub>4</sub>Ru<sub>4</sub>(CO)<sub>12</sub> adsorbed on magnesia and treated at 100 °C under He and very similar to the spectra observed by Guglielminotti for Ru<sub>3</sub>(CO)<sub>12</sub> on magnesia.<sup>20</sup> The spectra of FeRu<sub>3</sub> is similar to that observed by Basset and Shore on reacting H<sub>2</sub>FeRu(CO)<sub>12</sub> with hydrated magnesia.<sup>21</sup> However, more dramatic is the difference in thermal behavior. The FeRu<sub>3</sub> cluster has drastically changed by 200 °C and has completely disappeared by 300 °C. The Ru<sub>4</sub> cluster is considerably more robust maintaining most of its features to 300 °C.

We then started with fresh samples and studied their IR behavior in flowing 5% methane in argon to simulate the conditions that we use in our dehydrocoupling experiments. The results were quite dramatic and are shown in Figure 2. The spectra are shown starting at 25 °C on the bottom left. Here clearly the FeRu<sub>3</sub> cluster begins to interact with the methane even at room temperature, while the Ru<sub>4</sub> has the identical spectra to that observed under nitrogen. Notice the increased intensity of the absorption, here over 6 units while under nitrogen the spectra of FeRu<sub>3</sub> had an intensity of less than 0.2 units, and also the loss of features (compare to upper left spectra of Figure 1). This broad absorption band is similar to a feature observed by Guzzi<sup>22</sup> that was attributed to mobile subcarbonyls which arise from decomposition of the cluster. However, by 400 °C the two spectra have become identical (bottom right of Figure 2), a broad featureless absorption. This contrast to the spectra under nitrogen where by 400 °C both clusters and completely lost their absorption. We interpret these results as segregation of the metals. We hope next to study the C-H stretching region of the spectra to learn more about hydrocarbon fragments on the catalysts.

#### REFERENCES

1. J. A. Labinger, *Catalysis Letters* 1988, **1**, 371.
2. D. J. H. Smith, *Chimie-Raffinage* 1985, 10.
3. O. V. Bragin, T. V. Vasina, Ya. I. Isakov, B. K. Nefedov, A. V. Praobrazhenskii, N. V. Palishkina, and Kh. M. Minacher, *Izv. Akad. Nauk. SSSR, Ser. Khim.* 1982, (4), 954. CA Abstract 97:23370n.
4. S. S. Shepelev and K. G. Ione, *Kinet. Katal.* 1984, **25**(2), 347. CA Abstract 101:110432d.
5. T. Yamaguchi, A. Kadota, and C. Saito, *Chem Letters* 1988, 681.
6. A. H. P. Hall and J. J. McCarroll, U.S. Patent 1987, No. 4,695,663.
7. O. M. Gondouin, U.S. Patent 1987, No. 4,705,908.
8. H.L. Mitchell, III and R.H. Waghorne, U.S. Patent 1980, No. 4,239,658.
9. L. Devries and P. R. Ryason, U.S. Patent 1985, No. 4,507,517.
10. M.E. Dry and J.C. Hoogendoorn, *Catal. Rev.* 1981, **23**, 265.
11. D.L. King, J.A. Cusumano, and R.L. Garten, *Catal. Rev.* 1981, **23**, 203.
12. H.C. Foley, S.J. D-Cani, K.D. T Au, K.J. Chao, J.H. Onuferko, C. Dybowski, and B.C. Gates, *J. Am. Chem. Soc.* 1983, **105**, 3074.
13. J.P. Candlin and H. Thomas, "Supported Organometallic Catalysis", in *Homogeneous Catalysis II*, D. Forster and J.F. Roth, eds., *Adv. Chem. Series* 1974, **132**, 212-239.

14. Y.I. Yermakov, B.N. Kuznetsov, and V.A. Zakharou, "Catalysis by Supported Complexes," Vol.8, Studies in Surface Science and Catalysis, Elsevier, Amsterdam, (1981).
15. A.A. Bhattacharyya, C.L. Nagel, and S.G. Shore, *Organometallics* 1983, 2, 1187.
16. G.L. Geoffroy and W.L. Gladfelter, *J. Am. Chem. Soc.* 1977, 99, 7565.
17. J.J. Venter and M.A. Vannice, *Applied Spectroscopy* 1988, 42, 1096.
18. W. R. Moser, C.-C. Chiang, and R. W. Thompson, *J. Catalysis* 1989, 115, 532.
19. S. Uchiyama and B. C. Gates, *J. Catalysis* 1987, 110, 388.
20. E. Guglielminotti, *Langmuir* 1986, 2, 812.
21. A. Choplin, L. Huang, J.-M. Basset, R. Mathieu, U. Siriwardane, and S. G. Shore, *Organometallics* 1986, 5, 1547.
22. S. Dobos, I. Boxzormenyi, J. Mink, and L. Gucci, *Inorg. Chim. Acta* 1986, 120, 135 and 145.

Table 1

ACTIVITY OF RUTHENIUM CATALYSTS FOR METHANE DEHYDROGENATION<sup>a</sup>

Catalyst <sup>b</sup>	Ru (wt%)	Flow rate (mL/min)	Methane Conver (%)	% Selectivity <sup>c</sup> to		
				H <sub>2</sub>	C <sub>2</sub>	C <sub>6</sub> <sup>±</sup>
Ru-com	0.50	50	71.2	151.0	-- <sup>d</sup>	--
RuAL	0.35	10	3.0	139.9	2.8	--
RuMS	0.31	10	2.3	147.5	1.2	--
RuZL	0.37	10	1.7	177.5	2.6	--
Ru <sub>4</sub> AL	0.61	100	10.1	78.6	1.62	--
Ru <sub>4</sub> MS	0.49	100	4.9	146.6	3.52	--
Ru <sub>4</sub> ZL	0.61	50	1.7	25.3	6.9	28.9
Ru <sub>6</sub> AL	1.26	50	6.1	113.4	6.9	41.4
Ru <sub>6</sub> MS	0.19	50	5.6	192.8	1.0	14.8
Ru <sub>6</sub> ZL	0.20	50	3.6	161.9	3.6	10.0

<sup>a</sup>Reaction condition: temperature=750°C, pressure=150 psig

<sup>b</sup>Abbreviation: Ru-com=commercial ruthenium catalyst from Engelhard; Ru<sub>4</sub>=(C<sub>2</sub>H<sub>5</sub>)<sub>2</sub>AlRu<sub>4</sub>H<sub>3</sub>(CO)<sub>12</sub>; Ru<sub>6</sub>=(C<sub>2</sub>H<sub>5</sub>)<sub>2</sub>AlRu<sub>6</sub>H(CO)<sub>18</sub>; Ru=Ru (Allyl) (CO)<sub>2</sub>; AL=B- $\gamma$ -alumina; MS=5A molecular sieve; ZL=LZ-Y zeolite.

<sup>c</sup>Selectivities were calculated on converted methane. Selectivity to hydrocarbons are based on carbon number.

<sup>d</sup>Not detected.

Table 2  
ELEMENTAL ANALYSES OF RUTHENIUM CATALYSIS FOR METHANE  
REFORMING<sup>a</sup>

Catalyst	Before reaction			After reaction		
	%C	%H	%Ru	%C	%H	%Ru
Ru <sub>4</sub> AL	5.09	1.04	0.61	26.50	0.40	0.57
Ru <sub>4</sub> MS	1.46	1.13	0.49	4.38	0.46	0.64
Ru <sub>4</sub> ZL	5.25	1.53	0.61	0.58	0.22	1.26
Ru <sub>6</sub> AL	9.77	1.84	1.26	23.24	0.67	0.55
Ru <sub>6</sub> MS	0.95	1.68	0.19	22.29	0.19	0.32

<sup>a</sup>Reaction with methane at 750°C for 15 h.

Table 3  
EFFECT OF REACTION PRESURE AND SPACE VELOCITY TO  
THE ACTIVITY OF Ru<sub>6</sub>ZL<sup>a</sup> AT 750°C

Pressure (psig)	Flow rate mL/min	%CH <sub>4</sub> conversion	%Selectivity <sup>b</sup> of		
			H <sub>2</sub>	C <sub>2</sub>	C <sub>6+</sub>
50	50	3.18	164.16	6.04	6.6
150	50	5.19	91.33	4.48	10.70
250	50	8.64	82.41	2.46	7.38
250	100	2.62	177.10	9.24	20.64

<sup>a</sup>Ru<sub>6</sub>ZL = zeolite supported Ru<sub>6</sub> cluster, C<sub>2</sub>H<sub>5</sub>AlRu<sub>6</sub>H(CO)<sub>18</sub>.

<sup>b</sup>Selectivity was based on carbon number of hydrocarbon and the amount of methane reacted.

Table 4  
CATALYTIC REACTIVITY OF ZEOLITE AND MAGNESIA  
SUPPORTED CATALYSTS FOR METHANE DEHYDROGENATION<sup>a</sup>

Catalysts	Temp (°C)	Methane	Selectivity <sup>b</sup>	
		Conversion (%)	C <sub>2</sub> (%)	C <sub>6+</sub>
RuMgO	600	21.044	0.1	0.5
Ru <sub>4</sub> MgO	750	4.04	6.9	49.2
FeRu <sub>3</sub> ZL	600	3.07	1.9	18.5
FeRu <sub>3</sub> MgO	600	8.87	0.1	--

<sup>a</sup>Reaction conditions: pressure=150psig, flow rate=20 mL/min, weight of catalyst=2 g, reactor O.D.=3/8in (S.S.).

<sup>b</sup>Selectivity to hydrocarbon is based on carbon number.

<sup>c</sup>Not detected.

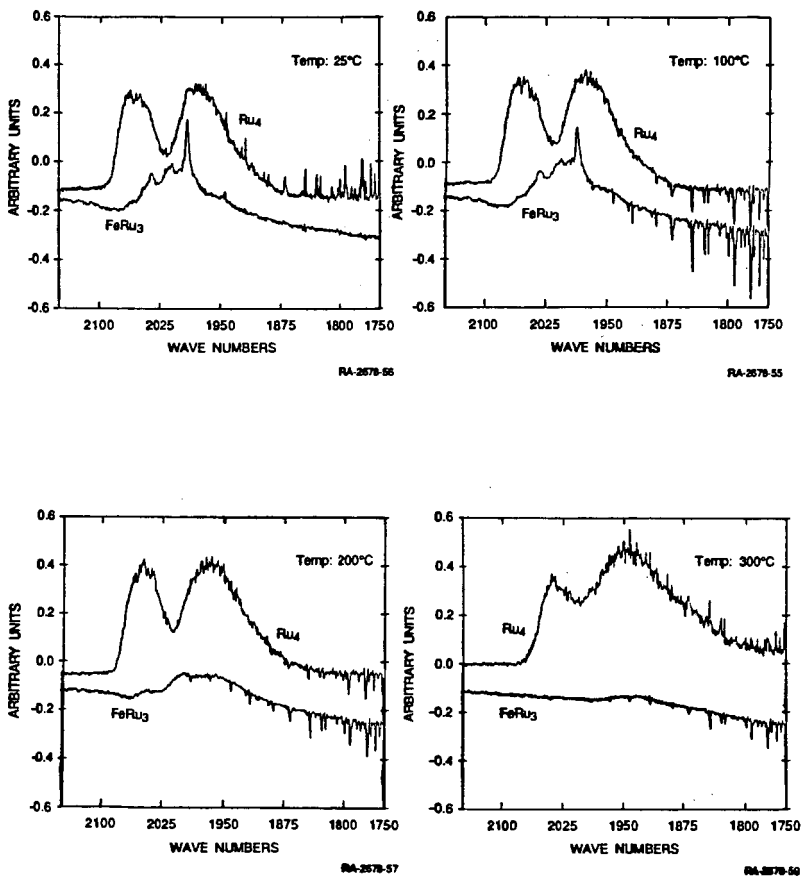
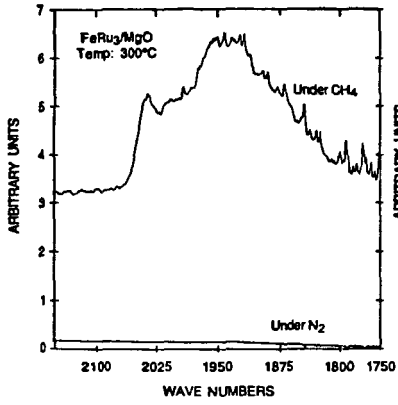
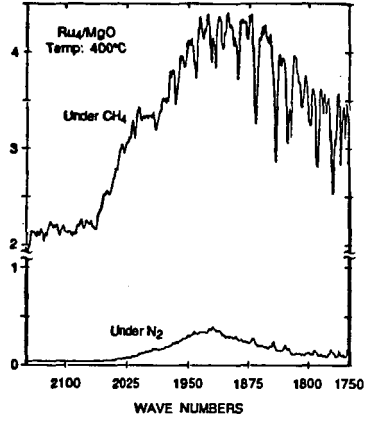


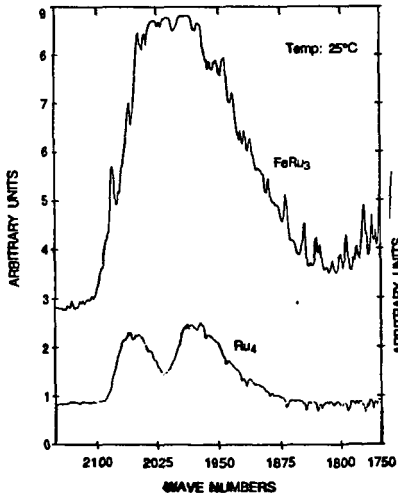
FIGURE 1: COMPARISON OF Ru<sub>4</sub> AND FeRu<sub>3</sub> CLUSTERS ON MgO UNDER N<sub>2</sub>.



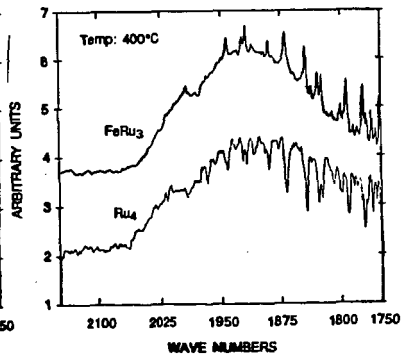
RA-2678-62



RA-2678-60



RA-2578-63



RA-2578-61

FIGURE 2: COMPARISON OF Ru<sub>4</sub> AND FeRu<sub>3</sub> CLUSTERS ON MgO UNDER CH<sub>4</sub>.

Oxidative Coupling of Methane over Perovskite-Type Oxides and Correlation of  
 $T_{\max}$  for Oxygen Desorption with  $C_2$  Selectivity

by

Abolghasem Shamsi\* and Khurram Zahir<sup>21</sup>

United States Department of Energy

Morgantown Energy Technology Center (METC)

P.O. Box 880

Morgantown, WV 26507-0880

ABSTRACT:

Oxidative coupling of methane co-fed with oxygen to  $C_2+$  hydrocarbons has been investigated both in the absence and in the presence of  $La_{0.9}Na_{0.1}MnO_3$  at 1 and 3.6 atm pressures. It was found that residence time, temperature, methane-to-oxygen ratio, and pressure are the major factors affecting the conversion and selectivity both in the empty reactor and in the presence of the catalyst. Significant gas-phase reactions were observed at higher pressure,  $O_2:CH_4$  ratio, and contact time. The results suggest that the activation of methane occurs both in the gas phase and on the surface of the catalyst, and the surface reactions appeared to be important in oxidizing the intermediates  $CH_3$ ,  $C_2H_4$ ,  $C_2H_6$ , and CO to carbon dioxide. Temperature-Programmed desorption studies on a series of perovskite-type catalysts showed that  $T_{\max}$ , the temperature at which maximum  $O_2$  desorbs, correlates very well with the  $C_2$  selectivity for oxidative coupling of Methane; and these results suggest that a strong binding of oxygen to the surface site is essential to selectively produce  $C_2+$  hydrocarbons from methane as opposed to complete oxidation leading to carbon dioxide.

#### BACKGROUND:

Methane is the principal component of natural gas, which is found in porous reservoirs generally associated with crude oil. Some of these abundant reserves of natural gas exist in locations too remote from market areas to be recovered on a commercial basis by present methods. A promising new methane conversion technology uses catalytic oxidative coupling as the first step in the process.<sup>1-3</sup> The oxidative coupling step converts natural gas to olefins, which could be subsequently converted to higher hydrocarbons.<sup>4</sup> A key to developing this technology is optimization of the oxidative-coupling step, such as using novel catalysts. We have shown that by proper cation substitution in perovskite-type oxides, superior catalysts for the oxidative coupling of methane to higher hydrocarbons can be obtained.<sup>5,6</sup> Recent studies showed that gas-phase reactions, especially at higher pressures, play a significant role in the partial oxidation of methane.<sup>7-9</sup> Furthermore, there appears to be a discrepancy between the results obtained by Ito et al.<sup>10</sup> and the results obtained by Yates and Zlotin<sup>7</sup> for empty reactors. Therefore, in order to gain further insight into this catalytic and noncatalytic system, the oxidative coupling of methane was investigated at several reaction conditions, both in the presence and absence of the perovskite-type oxide  $\text{La}_{0.9}\text{Na}_{0.1}\text{MnO}_3$ .

One of the most important factors which govern the catalytic oxidation process is the metal-oxygen bond strength.<sup>11</sup> For metal oxide catalysts, usually three different types of oxygen may be detected, namely, lattice oxygen, adsorbed

oxygen and absorbed oxygen.<sup>12</sup> These activated oxygen species have widely different properties in catalytic oxidation and can affect the activity of a particular catalyst. In the case of metal oxide catalysts, reactivity of these oxygen species depends largely upon the kind of component metal cation present.

Temperature-Programmed Desorption (TPD) is one of the techniques that can be used to obtain useful information on the existence of oxygen species in discrete states and/or over a broad distribution of energies.<sup>12-14</sup> Such information when combined with the results of catalytic reaction studies, carried out under identical conditions, can provide an insight into the catalytic-oxidative conversion of methane to hydrocarbons. In this paper, we report the oxygen-sorptive properties of perovskite-type catalysts in relation to their catalytic activity and selectivity.

#### EXPERIMENTAL:

The details of preparing the perovskite-type oxides have been reported elsewhere.<sup>5</sup> A 0.235m long downflow alumina reactor tube (9.53mm o.d., 6.35mm i.d., calculated heated volume =  $2.0 \text{ cm}^3$ ) with a quartz thermowell was used as a fixed-bed reactor with 0.5 g of catalyst (-28/+48 mesh) held in place by quartz wool. Electronic mass flow controllers were used to feed methane (99.99%), oxygen (99.8%), and helium (99.999%). The reactor was electrically heated to reaction temperatures under a flow of helium. All transfer lines and valves were 316 stainless steel and held at 150 °C. Product analyses were performed by online gas chromatography (GC) and mass spectrometry (MS). The products were sampled but not analyzed until performance stabilized and this

never exceeded 30 minutes. Samples were analyzed for ethane, ethylene, propane, propylene, hydrogen, carbon oxides, formaldehyde, and water. A thermal conductivity detector was used with a 1m x 3.2mm o.d. stainless steel molecular sieve 5A column and a 3.7m x 3.2mm o.d. stainless steel Porapak Q (80/100 mesh) column at isothermal oven temperatures of 100 and 120 °C, respectively. Results are reported on a carbon-mol % basis (Table 1).

Temperature-programmed studies were performed by passing oxygen (99.8%) over the catalyst and raising the temperature from room temperature to 820 °C with a heating rate of 5 °C/min, and cooling the catalyst to room temperature under oxygen atmosphere. Any excess oxygen not consumed by the catalyst was then flushed out by using high purity He (99.999%). Oxygen desorption was performed by raising the temperature linearly (heating rate = 60 °C/min) with time and using high purity He (30 cm<sup>3</sup>/min) as carrier gas. Products were analyzed by online gas chromatography (GC) and mass spectrometry (MS). For the blank experiment, where no catalyst was present in the reactor, no appreciable traces of oxygen were detected.

#### RESULTS:

The oxidative coupling of methane co-fed with oxygen was studied in an empty alumina reactor with and without dead volume (Table 1). The results showed that extensive conversion of methane and oxygen occurred in the empty reactor, especially at higher pressures and contact times. The heated volume of the reactor was calculated to be 2.0 cm<sup>3</sup> with a contact time of 2.4 seconds at maximum dead volume. However, as the contact time was reduced (< 1 second), by

minimizing the dead volume in the reactor, the contribution from the gas-phase reaction was significantly reduced. Since we were not able to measure the exact volume of the reactor with the minimized dead volume, the contact time is reported as "< 1 second".

Pressure also appears to be an important factor affecting conversion and selectivity both in the gas phase and on the surface of the catalyst. For example, at 1.0 atm pressure and 740 °C (not shown in Table 1), about 1.5 % of the methane and about 1.7 % of the oxygen were converted to products (9% C<sub>2</sub>H<sub>4</sub>, 38% C<sub>2</sub>H<sub>6</sub>, 3% CO<sub>2</sub>, and 49% CO) in the empty reactor (contact time = 2.4 seconds and CH<sub>4</sub>:O<sub>2</sub> = 2:1). When the pressure was raised to 3.6 atm, the methane and oxygen conversions increased to 35.7 and 96.8 %, respectively. The product distribution in this case was 11.2% C<sub>2</sub>H<sub>4</sub>, 4.6% C<sub>2</sub>H<sub>6</sub>, 15.8% CO<sub>2</sub>, and 68.4% CO.

The effects of temperature and pressure on conversions and selectivity to C<sub>2</sub>+ hydrocarbons, over La<sub>0.9</sub>Na<sub>0.1</sub>MnO<sub>3</sub> catalyst, are shown in Figure 1. At 3.6 atm pressure and temperatures below 780 °C, higher methane and oxygen conversions and higher selectivity to C<sub>2</sub>+ hydrocarbons were observed compared to those at 1 atm. However, when the temperature increased the C<sub>2</sub>+ selectivity at low pressure (1 atm) increased to a maximum value, while at the higher pressure the C<sub>2</sub>+ selectivity slightly decreased. Furthermore, a higher molar ratio of C<sub>2</sub>H<sub>4</sub>:C<sub>2</sub>H<sub>6</sub> was observed at higher pressure. In the presence of the catalyst, the major portion of the carbon oxides was carbon dioxide, indicating that the catalyst played a significant role in the reaction sequences and altered the product distribution.

The dependence of conversion and selectivity on the methane-to-oxygen ratio over  $\text{La}_{0.9}\text{Na}_{0.1}\text{MnO}_3$  was also studied (Figure 2.). Lower conversion of methane and higher selectivity to  $\text{C}_2+$  hydrocarbons were obtained when the methane-to-oxygen ratio was increased. This result indicates that methane and higher hydrocarbon products, at higher oxygen partial pressures and in the presence of the catalyst, were increasingly converted to carbon dioxide.

#### Temperature-Programmed Desorption:

Temperature-Programmed desorption studies on a series of perovskite-type catalysts with general formula  $\text{A}_{1-x}\text{B}_x\text{MnO}_3$  (where A is Gd, Sm, La, or Ho, B is either Na or K and  $x = 0$  or  $0.1$ ) were carried out and the temperature at which maximum oxygen desorbed ( $T_{\text{max}}$ ) was correlated with the  $\text{C}_2$  selectivity. The TPD chromatograms for oxygen desorption are shown in Figure 3 as plots of mass spectrometer signal (desorption rate) for oxygen ( $m/e = 32$ ) versus temperature. All chromatograms are characterized by the appearance of two types of oxygen. The first type, ( $\alpha$ ) oxygen, desorbs at a lower temperature compared to the second type, ( $\beta$ ) oxygen, which desorbs at higher temperature. The values for  $T_{\text{max}}$ , corresponding to the maxima for ( $\alpha$ ) oxygen desorption, are plotted in Figure 4 along with the  $\text{C}_2$  selectivities obtained in the earlier studies.<sup>6</sup> The values for  $T_{\text{max}}$  ranges from  $860^\circ\text{C}$  for  $\text{Gd}_{0.9}\text{Na}_{0.1}\text{MnO}_3$  to  $695^\circ\text{C}$  for  $\text{LaMnO}_3$  and is sensitive to the presence of alkali metal ion B as well as to substitution at site A.

The results presented in Figure 4 show that  $T_{\text{max}}$  for ( $\alpha$ ) oxygen desorption correlates very well with the  $\text{C}_2$  selectivity. The catalyst  $\text{Gd}_{0.9}\text{Na}_{0.1}\text{MnO}_3$  with

( $\alpha$ ) oxygen desorbing at the highest temperature (865 °C) showed the highest selectivity for C<sub>2</sub> products whereas LaMnO<sub>3</sub> which desorbs at the lowest temperature (695 °C) is the least selective for the conversion of methane to C<sub>2</sub> products.<sup>5</sup> It is interesting to note that optimum conditions (higher C<sub>2</sub> selectivity) for conversion of methane over La<sub>0.9</sub>Na<sub>0.1</sub>MnO<sub>3</sub> catalyst correspond to the temperature (820 °C) which matches very nicely with the T<sub>max</sub> for that catalyst. For the perovskite-type catalysts examined, it has been speculated earlier that the oxygen binding energy decreases in this order (La,Na)MnO<sub>3</sub> > (La,K)MnO<sub>3</sub> > (La,[])MnO<sub>3</sub>.<sup>15</sup> Present TPD studies provide an experimental basis for that trend in oxygen binding energies for these compounds and also similar information on other catalysts. For example, when comparing LaMnO<sub>3</sub> with La<sub>0.9</sub>K<sub>0.1</sub>MnO<sub>3</sub> and La<sub>0.9</sub>Na<sub>0.1</sub>MnO<sub>3</sub>, it becomes apparent that it is the nature of metal-oxygen bond that controls the catalytic activity of oxide catalysts. Therefore we suggest that in catalytic oxidation of methane to higher hydrocarbons, the most important factor may very well be the binding energy of oxygen to a surface site of the catalyst. This observation also agrees well with the earlier claim that some of the common selective oxidation catalysts (e.g. V<sub>2</sub>O<sub>5</sub>, MoO<sub>3</sub> and Bi<sub>2</sub>MoO<sub>6</sub>) did not contain weakly adsorbed oxygen.<sup>13</sup>

#### CONCLUSIONS:

We have shown that by proper cation substitution in perovskite-type oxides, superior catalysts for the oxidative coupling of methane to higher hydrocarbons can be obtained. The results show that surface reactions are important in oxidizing the intermediates CH<sub>3</sub>·, C<sub>2</sub>H<sub>4</sub>, C<sub>2</sub>H<sub>6</sub>, and CO to carbon dioxide. It was found that contact time, temperature, methane-to-oxygen ratio

and pressure were the major factors affecting the conversion and selectivity in the presence and absence of the catalyst. Furthermore, the high activity observed by Yates and Zlotin<sup>7</sup> for the empty reactor could be a result of the higher contact time and possible back pressure (caused by the capillary tube) when compared with the results reported by Ito et al.<sup>10</sup> The activation of methane appeared to be occurring both in the gas phase and on the surface of the catalyst. In the gas phase, methane was possibly activated by diatomic oxygen. The oxidation of methane in the gas phase by diatomic oxygen has been discussed in other reports.<sup>16,17</sup>

The types of oxygen species on the surfaces of the catalyst responsible for the activation of methane are not well defined. However, the activation of methane by surface oxygen species has been proposed by several researchers. Liu et al.<sup>18</sup> have shown  $O^-$  ions; Driscoll et al.<sup>19</sup> have proposed  $[Li^+O^-]$  centers; and Otsuka and Jinno<sup>20</sup> have proposed adsorbed diatomic oxygen, as being responsible for the activation of methane.

From the TPD studies, we can conclude that for the perovskite-type catalysts examined, a strong binding of oxygen to the surface site is essential to selectively produce  $C_2+$  hydrocarbons from methane as opposed to complete oxidation leading to undesirable carbon dioxide. Present results suggest a possibility that TPD technique can be utilized to find more effective catalysts by selecting a proper combination of A and B site substitution in perovskite-type catalysts.

REFERENCES:

- (1) Ekstrom, A.; Lapszewicz, J. A. *J. Am. Chem. Soc.* 1988, 110, 5226.
- (2) Labinger, J. A.; Ott, K. C. *J. Phys. Chem.* 1987, 91, 2682.
- (3) Zhang, H.-S.; Wang, J.-X.; Driscoll, D.; Lunsford, J. H. *J. of Catal.* 1988, 112, 366.
- (4) Jezl, J. L.; Michael, G. O.; Spangler, M. J. U.S. Patent 1988, 4,754,091, June 28.
- (5) France, J. E.; Shamsi, A.; Ahsan, M. O. *Energy & Fuels* 1988, 2(2), 235.
- (6) France, J. E.; Shamsi, A.; Headley, L. C.; Ahsan, M. O. *Energy Progress* 1988, 2(4), 185.
- (7) Yates, D. J. C.; Zlotin, N. E. *J. of Catal.* 1988, 111, 317.
- (8) Lane, G.; Wolf, E. E. *J. of Catal.* 1988, 113, 144.
- (9) Asami, K.; Omata, F.; Fujimoto, K.; Tominaga, H. O. *J. Chem. Soc. Commun.* 1987, 1287.
- (10) Ito, T.; Wang, J.-X.; Lin, C.-H.; Lunsford, J. H. *J. Am. Chem. Soc.* 1985, 107, 5062.
- (11) Kung, H. H. *Ind. Eng. Chem. Prod. Res. Dev.* 1986, 25, 171.
- (12) Seiyama T.; Yamazoe, N.; Eguchi, K. *Ind. Eng. Chem. Prod. Res. Dev.* 1985, 24, 19.
- (13) Iwamoto M.; Yoda, Y.; Yamazoe, N.; Seiyama, T. *J. Phys. Chem.* 1987, 82, 2654.
- (14) Falconer J. L.; Schwartz, J. A. *Catal. Rev. Sci. Eng.* 1983, 25, 141.
- (15) Voorhoeve R. J. H.; Remeika, J. P.; Trimble, L. E.; Cooper, A. S.; Disalvo, F.J.; Gallagher, P. K. *J. Solid State Chem.* 1975, 14, 395.
- (16) Bone, W. A. *Proc. R. Soc. London, Ser. A* 1932, 137, 243.

- (17) Walker, R. W. *Reaction Kinetics*; The Chemical Society Burlington House, London, 1975; Vol.1, pp 161-211.
- (18) Liu, H.-F.; Liu, K. Y.; Johnson, R. E.; Lunsford, J. H. *J. Am. Chem. Soc.* 1984, 106, 4117.
- (19) Driscoll, D. J.; Martir, W.; Wang, J.-X.; Lunsford, J. H. *J. Am. Chem. Soc.* 1985, 107, 58.
- (20) Otsuka K.; Jinno, K. ; Morikawa, A. *J. of Catal.* 1986, 100, 353.
- (21) Oak Ridge Associated Universities Postdoctoral Research Fellow

Table 1. Comparison of Activity and Selectivity of Oxidative Coupling of Methane in the Presence and Absence of Catalyst at 845 °C, Alumina Reactor, CH<sub>4</sub>/He/O<sub>2</sub>=20/20/10 cm<sup>3</sup>/min NPT flow rates.

Catalyst/ Conditions	Conversion (mol%)		Selectivity (carbon-mol%)			
	Methane	Oxygen	C <sub>2</sub> H <sub>4</sub>	C <sub>2</sub> H <sub>6</sub>	CO <sub>2</sub>	CO
Empty, Contact time 2.4 seconds, 1 atm.	29.9	62.9	19.0	5.7	8.8	66.5
Empty, Contact time < 1 second, 1 atm.	1.0	0.5	34.8	51.5	1.2	12.5
Empty, Contact time < 1 second, 3.6 atm.	18.5	37.7	21.8	12.4	8.9	56.9
La <sub>0.9</sub> Na <sub>0.1</sub> MnO <sub>3</sub> , 0.5 g, Contact time 0.4 second, 1 atm.	19.8	44.5	30.0	17.4	41.5	11.1
La <sub>0.9</sub> Na <sub>0.1</sub> MnO <sub>3</sub> , 0.5 g, Contact time 2.4 seconds, 1 atm.	37.2	85.1	36.6	13.7	43.2	6.5

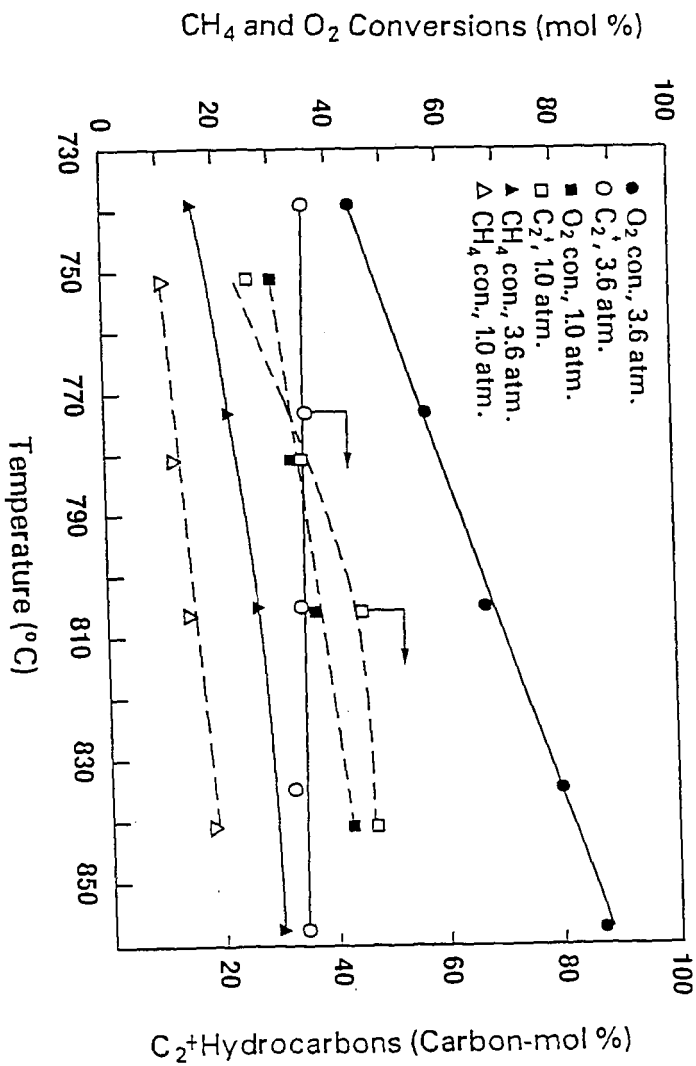
Figure captions:

Figure 1. Dependence of conversion and selectivity on temperature and pressure over  $\text{La}_{0.9}\text{Na}_{0.1}\text{MnO}_3$  Catalyst:  $\text{CH}_4/\text{He}/\text{O}_2 = 20/20/10$  NPT flow rates; contact time = 0.4 seconds; 0.5 g catalyst.

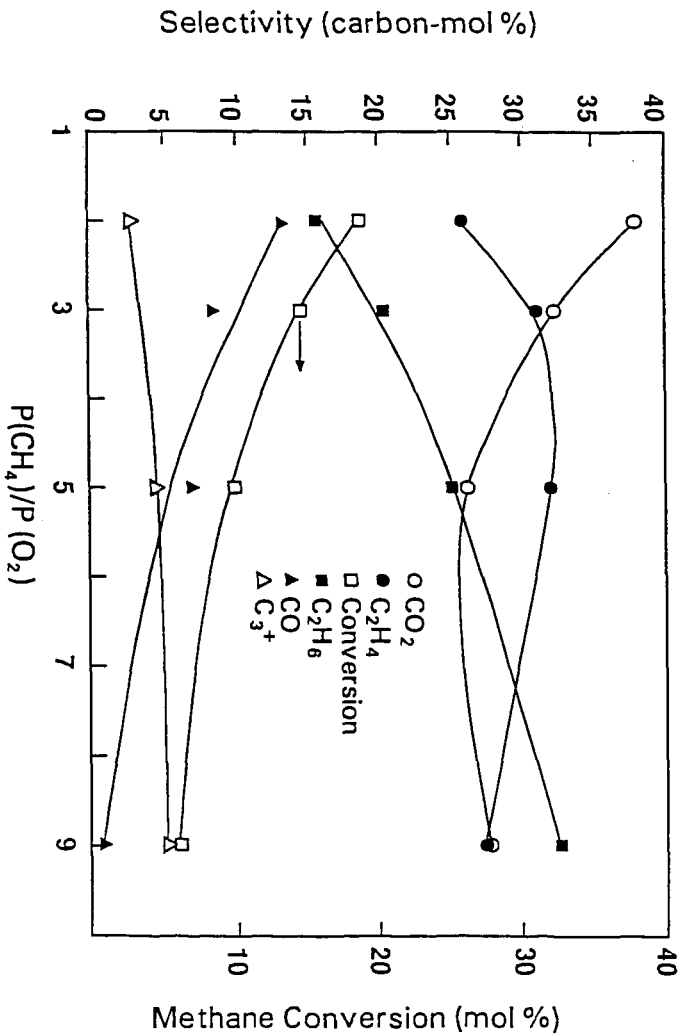
Figure 2. The effect of methane-to-oxygen ratio on conversion and selectivity over  $\text{La}_{0.9}\text{Na}_{0.1}\text{MnO}_3$  in an alumina reactor: 1.0 atm pressure; 830 °C;  $\text{CH}_4/\text{He}/\text{O}_2 = 20/20/10$  NPT flow rates; contact time = 0.4 second; 0.50 g catalyst.

Figure 3. Temperature-programmed desorption of oxygen ( $m/e = 32$ ): Heating rate = 1 °C/sec., He flow rate = 0.5  $\text{cm}^3/\text{sec.}$ , 0.25 g catalyst.

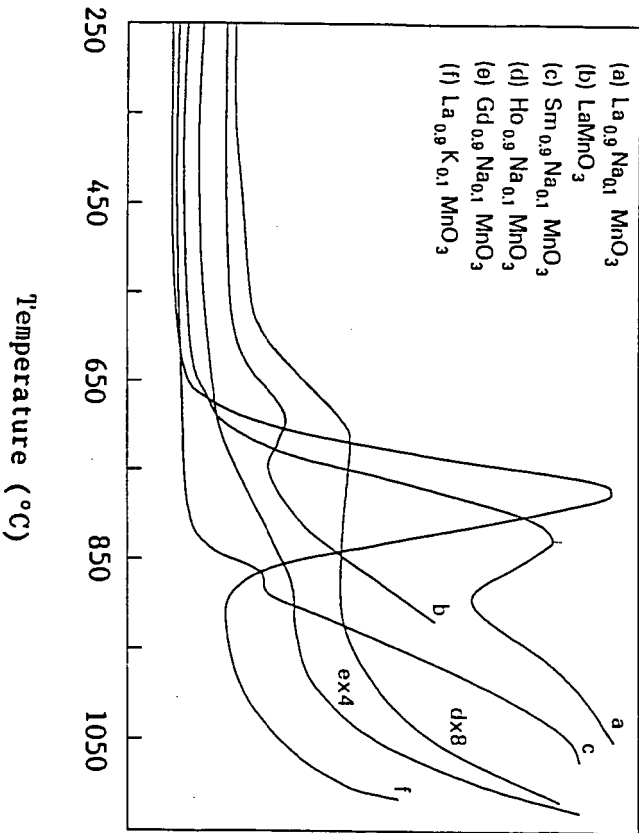
Figure 4. Correlation of  $\text{C}_2$  Selectivity with the temperature at which maximum  $\text{O}_2$  desorbs ( $T_{\text{max}}$ ): 0.25 g catalysts tested at 820 °C,  $\text{CH}_4/\text{O}_2$  ratio = 5.

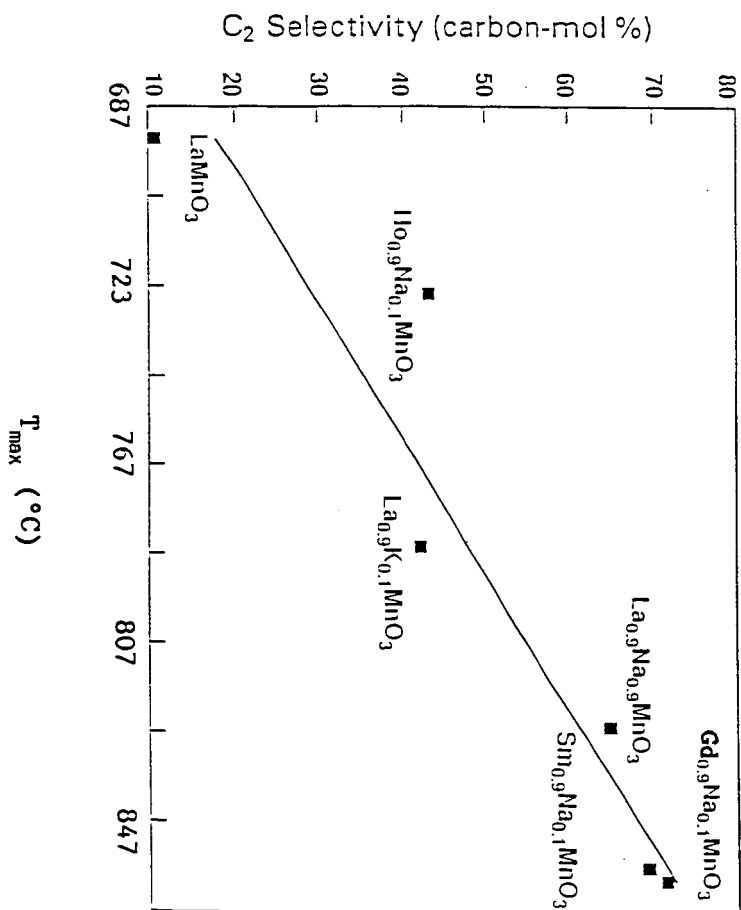


CB9-467-E AA3



Desorption Rate  $\rightarrow$





PHOTOCHEMICALLY-DRIVEN BIOMIMETIC OXIDATION  
OF ALKANES AND OLEFINS

J. A. Shelnut, D. E. Trudell  
Fuel Science Division 6211  
Sandia National Laboratories, Albuquerque, NM 87185

ABSTRACT

A photochemical reaction for oxidation of hydrocarbons that uses molecular oxygen as the oxidant is described. A reductive photoredox cycle that uses a tin(IV)- or antimony(V)-porphyrin photosensitizer generates the co-reductant equivalents required to activate oxygen. This "artificial" photosynthesis system drives a second catalytic cycle, mimicking the cytochrome  $P_{450}$  reaction, which oxidizes hydrocarbons. An iron(III)- or manganese(III)-porphyrin is used as the hydrocarbon-oxidation catalyst. Methylviologen can be used as a redox relay molecule to provide for electron-transfer from the reduced photosensitizer to the Fe or Mn porphyrin, but appears not to enhance efficiency of the process. The system is long-lived and may be used in time-resolved spectroscopic studies of the photo-initiated reaction to determine reaction rates and intermediates.

INTRODUCTION

Many alkane and olefin oxidation systems that mimic biological oxidation of hydrocarbons by cytochrome  $P_{450}$  have been reported. Most use an iron, manganese, or ruthenium porphyrin as the analog of the heme (iron porphyrin) functional group of the enzyme.<sup>1-8</sup> In the great majority of these chemistries a single oxygen atom donor, such as iodosylbenzene or hypochlorite, is used as the oxidant rather than molecular oxygen.<sup>1-4</sup> When molecular oxygen is used as the oxidant, as is the case for cytochrome  $P_{450}$ , reducing equivalents must be supplied to reduce the Fe porphyrin causing it to bind and split dioxygen and, subsequently, oxidize the alkane substrate. Several biomimetic systems have been demonstrated using either sodium borohydride, hydrogen/Pt, ascorbate, or zinc metal as the co-reductant.<sup>5-8</sup>

We have been investigating these reactions from the standpoint of stereochemically controlling the reaction at the metal site by designing metalloporphyrins with a shape- and size-selective pocket at the metal center.<sup>9,10</sup> The pockets designed so far are small, and thus require an oxidant, like  $O_2$ , that is small enough to enter the cavity. It is also desirable that the system be stable and operate over many hours. We are interested also in the possibility of photo-initiating the reaction so that reaction intermediates can be followed using time-resolved spectroscopic techniques for kinetic studies. This can be accomplished if the reductant is the product of a photoredox cycle.

Here we describe such a photochemically driven system for oxidation of alkanes and olefins. The system is illustrated in Figure 1. The cycle on the left is the photoredox chemistry that produces the reductant, a long-lived tin(IV)-porphyrin radical anion. In the cycle, a tin(IV)- or antimony(V)-porphyrin absorbs a photon of visible light resulting in the formation of the triplet excited state of the porphyrin. The porphyrin photosensitizer in its excited state is reduced by a sacrificial electron donor such as triethanolamine (TEOA).<sup>11-13</sup> The resulting long-lived  $\pi$  anion of the porphyrin has a

redox potential low enough to reduce either a Fe(III) or Mn(III) porphyrin, which acts as a catalyst for the biomimetic oxidation of hydrocarbons.<sup>13,14</sup> After reduction of the FeP, the photosensitizer anion (SnP<sup>-</sup>) returns to the resting redox state (SnP). Actually, two molecules of the porphyrin anion are required in the biomimetic P<sub>450</sub> cycle as indicated in Figure 1; the first to reduce Fe(II) to Fe(III), allowing O<sub>2</sub> to bind and a second to split dioxygen to form the reactive O=FeP intermediate. In some cases a molecule such as heptylviologen (HV<sup>2+</sup>) is used to relay the electron from the SnP anion to the P<sub>450</sub> cycle. Acetic or benzoic anhydride is sometimes used as an oxygen atom acceptor (replacing H<sup>+</sup>) in the splitting of dioxygen in the hydrocarbon (RH) oxidation cycle.

## RESULTS AND DISCUSSION

A photochemical reaction like that illustrated in Figure 1 was carried out in acetonitrile under an O<sub>2</sub> or air atmosphere. In a typical reaction, 0.24 μmol of Fe(III) tetra(pentafluoro-phenyl)porphyrin (FeTF<sub>5</sub>PP) chloride, 0.45 μmol of Sn(IV) protoporphyrin IX (SnProtoP) dichloride, 1.1 mmol of TEOA, 1.4 μmol of heptylviologen (N,N'-diheptyl-4,4'-dipyridinium dichloride), and 11 μmol of benzoic (or acetic) anhydride, were added to 1 ml of acetonitrile. Hexane (4.7 mmol) was added as a substrate. The samples, contained in a 1-cm path length cuvette, were irradiated with a tungsten lamp for 1-6 hr. Light of wavelengths less than 380 nm was filtered to insure that photosensitization of the reaction was only due to visible light absorption by the porphyrin. 1-, 2-, and 3-Hexanol and 2- and 3-hexanone products were quantified at the end of the run by gas chromatography. Table 1 gives yields and hexanol to hexanone product ratios for typical runs and control experiments.

In the presence of the P<sub>450</sub> catalyst, a generally higher overall yield of products is observed when illumination and other conditions were identical; however, a lower average hexanol to hexanone ratio of 1.3:1 is observed. However, in the absence of the catalyst FeTF<sub>5</sub>PP, photosensitized production of hexanols and hexanones is observed in an average ratio of 2.3:1. In the absence of O<sub>2</sub>, light, photosensitizer, or triethanolamine, there is no significant yield of oxidized hexane.

It is apparent that more than one oxygen activation pathway exists. The excited triplet state of tin porphyrins is known to be quenched in the presence of O<sub>2</sub>,<sup>14</sup> suggesting a possible direct mechanism of O<sub>2</sub> activation by the photosensitizer. We have examined reactions of both singlet O<sub>2</sub> and superoxide anion under our reaction conditions. Chemically-produced superoxide (KO<sub>2</sub>/18-crown-6) is not reactive under our experimental conditions. On the other hand, singlet oxygen, produced by irradiation of free base protoporphyrin (H<sub>2</sub>ProtoP),<sup>15</sup> is reactive in the presence of tertiary amines and gives about the same hexanol to hexanone ratio (2.7, see Table 1) as is observed in the presence of the SnP photosensitizer. Sn-, Sb-, and H<sub>2</sub>ProtoP all have triplet lifetimes of 10 ms or longer, and form singlet O<sub>2</sub> by intermolecular triplet-triplet annihilation. In fact, the photophysical parameters and singlet oxygen sensitizing properties of SnProtoP<sup>14,16</sup> are similar to metal-free porphyrins.<sup>17</sup> The similarity of photosensitizing characteristics of Sn-, Sb-, and H<sub>2</sub>-porphyrins explains the similarity of their properties in the FeP-free reaction (Table 1). However, only the Sn and Sb porphyrins form the stable anions capable of driving the Fe-porphyrin catalyzed reaction.

In the presence of the iron-porphyrin, the alcohol/ketone product

ratio is modified (-ol/-one  $\approx$  1) indicating that a competing reaction comes into play. If the FeP-catalyzed reaction is to account for the low product ratio, then this reaction necessarily must give a lower hexanol to hexanone ratio. We can test this hypothesis by determining the product ratio for the  $P_{450}$  cycle when driven by addition of a suitable reductant in the absence of light. Table 1 includes the yield and product ratio for the dark reaction of hexane and  $O_2$  catalyzed by  $FeTF_3PP$  using a Zn/Hg amalgam as the co-reductant.<sup>18</sup> (The ranges of yields and product ratios are for a range of solution conditions. The reaction is run for 2 hr, but is complete in about 10 min in most cases. Although the yields in some cases represent less than one catalyst turnover, the reaction can be continued by adding more amalgam. The FeP or MnP catalyst is required for significant yields of oxidized hexane. In some cases methylviologen is used as a relay molecule, and acetic anhydride is used as an oxygen atom acceptor. The product yield is sensitive to the amount of water in the acetonitrile solvent, and, in addition, acetic acid improved the overall yield and raised the alcohol/ketone product ratio. Presumably, acetic acid aids in the dioxygen lysis step in the reaction.)

Most importantly, when the FeP catalyst is present in the dark reaction the product ratio is one or less. Therefore, the dark reaction appears to compete favorably with the formation of singlet  $O_2$  and the photochemical reaction proceeds as shown in Figure 1. The dark reaction, which also occurs in the presence of light, results in the observed lowering in the alcohol/ketone ratio and higher yield measured for the light-driven reaction in the presence of the FeP catalyst. Also, viologen appears not to aid the reaction, since the yield generally remains unchanged or is slightly lowered in its presence (data not shown).

When cyclohexene is the substrate in the dark reaction, the products cyclohexene oxide (1.0), 2-cyclohexen-1-ol (2.2), and 2-cyclohexen-1-one (1.8) are observed in the ratios (relative product yields are given in parenthesis) observed in other dioxygen-based systems that mimic the cytochrome  $P_{450}$  reaction.<sup>19,20</sup> Also, when Mn tetraphenyl porphyrin is used as the catalyst, imidazole binding as a fifth ligand acts as a promoter for  $P_{450}$  reaction as has been noted in earlier studies.<sup>21</sup> Both of these results support the contention that the reaction is occurring at the porphyrin catalyst under these solution conditions.

The photochemical system produces stable yields of hydrocarbon oxidation products for more than 6 hr as shown in Figure 2. In Figure 2, the yield of products is given in terms of catalyst turnovers (mol product/mol FeP catalyst) as a function of reaction time. Also plotted in Figure 2 is the yield per hour, which only degrades slightly over the 6 hr reaction time. Finally, the alcohol/ketone ratio is a function of reaction time, increasing slightly as the reaction proceeds. The increase in the product ratio and decrease in oxidation rate both could be explained by slow degradation of the FeP-catalyzed cycle.

In summary, a photochemically driven reaction that mimics biological photosynthesis, electron-transfer, and hydrocarbon-oxidation reactions has been described. The reaction occurs at room temperature and uses  $O_2$  as the oxidant. Most importantly, the reaction can be run for hours without significant degradation. This means that the oxidation of low molecular weight alkanes by  $O_2$ , which proceeds at a lower rate than for hexane, can be investigated. Further studies are underway to determine the detailed reaction mechanisms involved in the photochemical reaction. Transient absorption and Raman spectroscopic techniques will also be applied to determine reaction rates.

#### ACKNOWLEDGEMENTS

This work performed at Sandia National Laboratories and supported by the United States Department of Energy Contract DE-AC04-76DP00789.

#### REFERENCES

1. For recent reviews see: (a) Ortiz de Montellano, P. R., Ed. "Cytochrome P-450; Structure, Mechanism, and Biochemistry" (Plenum: New York) 1986. (b) Guengerich, F. P.; Macdonald, T. L., *Acc. Chem. Res.* 1984, 17, 9.
2. Groves, J. T.; Nemo, T. E.; Myers, R. S., *J. Am. Chem. Soc.* 1979, 101, 1032.
3. Groves, J. T.; Quinn, R., *J. Am. Chem. Soc.* 1985, 107, 4343.
4. Colman, J. P.; Brauman, J. I.; Meunier, T.; Hayashi, T.; Kodadek, T.; Raybuck, S. A., *J. Am. Chem. Soc.* 1985, 107, 2000.
5. Tabushi, I.; Koga, N., *J. Am. Chem. Soc.* 1979, 101, 6456.
6. Perree-Fauvet, M.; Gaudemer, A., *J. Chem. Soc. Chem. Commun.* 1981, 874.
7. Tabushi, I.; Yazaki, A., *J. Am. Chem. Soc.* 1981, 103, 7371.
8. Fontecave, M.; Mansuy, D., *Tetrahedron* 1984, 40, 2847.
9. Shelnutz, J. A., Stohl, F. V.; Granoff, B., Preprints, Fuel Chem. Div., ACS, Los Angeles, CA, September 25-30, 1988.
10. Quintana, C. A.; Assink, R. A.; Shelnutz, J. A., *Inorg. Chem.* 1989, in press.
11. Shelnutz, J. A., *J. Am. Chem. Soc.* 1983, 105, 7179.
12. Shelnutz, J. A., *J. Phys. Chem.* 1984, 88, 6121.
13. Shelnutz, J. A., U. S. Patent 4,568,435, 1986.
14. Kalyanasundaram, K.; Shelnutz, J. A.; Grätzel, M., *Inorg. Chem.* 1988, 27, 2820.
15. (a) Cannistraro, S.; Jori, G.; Van de Vorst, A., *Photobiochem. Photobiophys.* 1982, 3, 353. (b) Cox, G. S.; Whitten, D. G., *Adv. Exp. Med. Biol.* 1983, 160, 279.
16. Land, E. J.; McDonagh, A. F.; McGarvey, D. J.; Truscott, T. G., *Proc. Natl. Acad. Sci. USA* 1988, 85, 5249.
17. Gouterman, M., in "The Porphyrins" Vol. 3, Dolphin, D., ed. (Academic: New York) Chpt. 1, 1978.
18. Karasevich, E. I.; Khenkin, A. M.; Shilov, E., *J. Chem. Soc., Chem. Commun.* 1987, 731.
19. Paulsen, D. R.; Ullman, R.; Soane, R. B.; Closs, G. L., *J. Chem. Soc., Chem. Commun.* 1974, 186.
20. Masui, M.; Tsuchida, K.; Kimata, Y.; Ozaki, S., *Chem. Pharm. Bull.* 1987, 35, 3078.
21. Battioni, P.; Renaud, J-P.; Bartoli, J. F.; Mansuy, D., *J. Chem. Soc., Chem. Commun.* 1986, 341.

TABLE 1. Oxidation of hexane by air in acetonitrile.

Catalyst	Reductant System	-ol/-one	Yield <sup>a</sup> (turnovers/hr)
FeTF <sub>5</sub> PP	SnProtoP, hν, TEOA	1.3 <sup>b</sup>	4.3
FeTF <sub>5</sub> PP	SbProtoP, hν, TEOA	1.0	0.8
FeTF <sub>5</sub> PP	hν, TEOA	0.8	0.2
MnTPP	SnProtoP, hν, TEOA	0.9	0.2
FeTF <sub>5</sub> PP	Zn/Hg	0.2-1.1	0.5-1.0 <sup>c</sup>
-	SnProtoP, hν, TEOA	2.3 <sup>b</sup>	1.7
-	H <sub>2</sub> ProtoP, hν, TEOA	2.7	0.6
-	SbProtoP, hν, TEOA	2.2	1.4 <sup>d</sup>
-	hν, TEOA	-	0.0
-	SnProtoP, hν	-	0.0

- a. Yield is in photosensitizer turnovers (mol product/mol photosensitizer) for selected runs. Catalyst concentrations are about one-half of the photosensitizer concentration.
- b. Hexanol/hexanone value is average for all (~20) runs with turnovers > 1.
- c. Total turnovers under various solvent conditions with O<sub>2</sub> as the oxidant.
- d. Light intensity higher than for SbProtoP/FeTF<sub>5</sub>PP run, accounting for higher yield in this case.

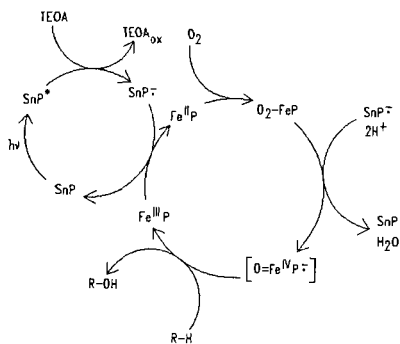


Figure 1. Scheme for photochemical production of co-reductant to drive the oxidation of hydrocarbons by mimicking the cytochrome-P<sub>450</sub> cycle. The SnP sensitized photoredox cycle is on the left; the P<sub>450</sub> catalytic cycle is shown on the right.

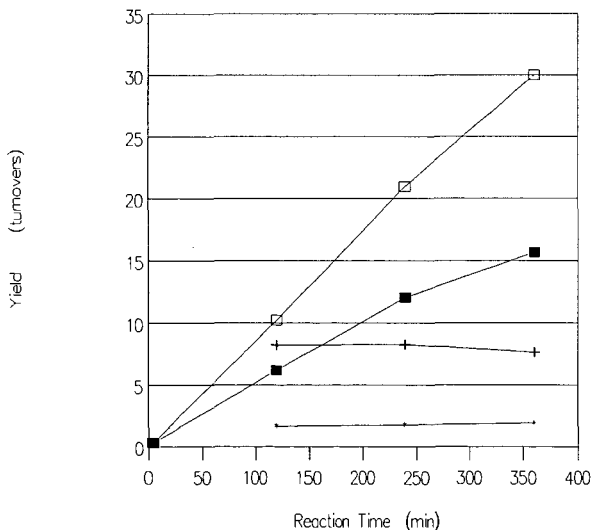


Figure 2. Hexanol and hexanone yields and product ratio as a function of reaction time. Total 1-, 2-, and 3-hexanol yield in catalyst turnovers (□); total 2- and 3-hexanone yield (■); hexanol/hexanone ratio (\*); catalyst turnovers/hr (+).

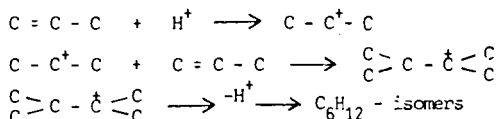
SYMPOSIUM ON NEW CATALYTIC MATERIALS  
PRESENTED BEFORE THE DIVISION OF FUEL CHEMISTRY  
AMERICAN CHEMICAL SOCIETY  
MIAMI MEETING, SEPTEMBER 10-15, 1989

OLIGOMERIZATION OF ISO-BUTENE WITH AN IMPROVED CATALYST

S. Börje Gevert, Peter Abrahamsson and Sven G. Järås  
Department of Engineering Chemistry 1,  
Chalmers University of Technology, Göteborg, S-412 96 Sweden

INTRODUCTION

In conversion processes in oil refining LPG (C<sub>3</sub> and C<sub>4</sub>) are formed as byproducts. When catalytic cracking is used the LPG will have a high content of unsaturated components. The low price of the LPG, compared to gasoline, makes oligomerization of the molecules in LPG worthwhile for the industry. There are mainly two processes used in the refineries for this purpose. In alkylation, liquid sulphuric or hydrofluoric acids are employed and in the other process phosphoric acid on silica or diatomeric earth. In the refining industry the latter process is normally called polymerization, although dimerization is the dominating and most wanted reaction. In the alkylation process iso-butene is reacted with either propane or butane. If using the less strong phosphoric acid, two alkenes must be used as reactants and at a higher temperature. The mounted phosphoric acid catalyst leaks less acid to downstream processing and therefore gives less severe corrosion problems than with alkylation (1). The chemistry of the oligomerization can be shown as:



The formed carbonium ions and hexenes can react further to trimers and higher. The phosphoric acid on silica catalyst is also an important catalyst for the production of petrochemical intermediates like nonene and alkylated aromates.

The traditional method of producing the mounted phosphoric acid on silica is to start from kieselguhr and phosphoric acid. The water content of the phosphoric acid should be low so that the final catalyst contains 65-70% by weight of P<sub>2</sub>O<sub>5</sub>. The mixture is extruded or bricketted, dried, calcined and finally hydrated to a preferred level, usually with steam. There are several proposals in the patent literature to improve the mechanical strength of the final product. One method is to steam treat the mixture before extrusion (2). It is also possible to add bentonite, montmorillonite, halloysite, or other compounds to the mixture before extrusion. The acidity of the catalyst can also be reached by using an aluminum silicate or zeolite instead of the above mentioned acids. The kieselguhr carrier can be replaced by a silica hydrogel (3,4). Recently Bernard et al (5) proposed to extrudate the silica carrier before impregnating the phosphoric acid. Little interest has been shown in the development of new or improved catalysts for oligomerization of propene and butene in the recent literature. It is therefore of interest to use modern analytical instruments to explain and improve the catalyst. In this paper, an improved catalyst based on mounted phosphoric acid on silica will be presented.

## EXPERIMENTAL

The used silica carriers were spheres with a diameter of 2.2 mm, received from Shell Corp. in London. In Table 1, more details of pore volumes and pore sizes are presented. The phosphoric acid used was of pro analysi quality from Kebo Lab. (Sweden) and the iso-butene from AGA Gas Ltd. (Sweden).

The catalysts were made by combining the following steps in different sequences: Impregnation with phosphoric acid of 42% by weight of  $P_2O_5$  or other concentrations if indicated. Drying at 170°C for 5 hrs. and calcining in a muffle furnace for 4 hrs. at various temperatures. Some catalysts were steamed at 100°C in 100% steam.

Testing of the activity of the catalysts was done in a 23 cc stainless steel reactor with iso-butene in vapour phase. A constant contact time of 1.00 hr. was maintained in all experiments by measuring and controlling the inlet flow. In Figure 1, a simple flow diagram of the reaction system is presented. Temperature, pressure and gas flow were kept constant at 160°C, 1 atm and 12.5 g of iso-butene per hour, respectively. The yields were determined by measuring the weight of liquid products and the amount of iso-butene feed. The liquid products were analyzed on GC with FID detector and the simulated distillation was made according to ASTM D2887-3. BET pore volume and surface area were measured with Micromeritics Digisorb 2600.

## RESULTS AND DISCUSSION

In Table 2, the BET surface area and pore volumes of the silica spheres used are presented. The pore volume determined with the BET method is considerably different from the pore volumes presented by the manufacturer of the silica spheres (Table 1). The main difference is probably due to macro pores not detected by the BET method.

Impregnation of the silica sphere I with different acid concentrations followed by drying at 170°C, did not effect the initial activity of the final catalyst. However, after 20 hrs. of experiment, catalyst produced by impregnating higher concentrations of phosphoric acid showed a lower conversion (Table 3). In spite of this it is important to use a higher concentration of the acid in order to reach a  $P_2O_5$  concentration of 65-70% in the final catalyst. On the other hand, too high a viscosity, which is found in concentrated phosphoric acid, reduces the impregnation speed.

In figure 2, the conversion as a function of time is presented for three different catalysts produced from the three different silica spheres by the same procedure. Calcination was done at 425°C. The catalyst produced from silica spheres III, with both larger pores and pore volume compared with silica spheres II, gives the highest activity. The conversion was 78% after 20 hrs. of experiment. The catalyst produced from silica sphere II, gives a better conversion than does the catalyst produced from silica sphere I. Thus the selection of silica carrier should be; large average pores and large pore volumes.

In Figure 3 the effect on activity of calcining at 350°C and 425°C is presented. The higher temperature gives a lower activity and calcining at 350°C gave a catalyst with a conversion of 97,6%. This catalyst also maintained the conversion level in an experiment of over 70 hrs. In a separate experiment silica spheres were calcined at 550°C, before impregnation without affecting the conversion of the final product. Calcining after impregnation effects the bindings between phosphoric acid and the

silanol groups and dehydration of the phosphoric acid. As no effect of calcining at 550°C before impregnation was noted, the silanol groups of the silica remained intact. If only one impregnation is carried out, the activity of the final catalyst drops quickly after a few hours of the experiment (Table 3). When water is added in the feed, or the catalyst is wetted with water, the activity rises again for a short period. This indicates that the phosphoric acid bound to the silica is not as active as free acid in the catalyst. It is probably due to the fact that bound acid does not have the same capacity to retain water as free acid. The high sensitivity of water content in the feed makes the catalyst, which has been impregnated once only, impractical for commercial use.

In Figure 4 the activity of commercial catalyst is plotted as a function of time. The ground catalyst shows a much higher conversion rate (66%) after 20 hrs of experiment than the unground catalyst (18%). In the small reactor used, the unground catalyst will give large wall effects due to the small dimensions of the reactor. The ground catalyst has a lower activity compared to the best of the catalysts produced in this study. In the production of gasoline a dimer or trimer is wanted, while the formation of tetramers is not wanted since they normally fall outside the gasoline boiling range. The selectivity of some catalysts is presented in Table 4. For catalysts with high conversions, the formation of tetramers is also high. The catalyst calcined at 350°C shows an acceptable selectivity (dimer + trimer = 96%) and at the same time conversion 98%. The unground commercial catalyst shows 4.3% tetramers in the liquid while the ground catalyst only shows 2.8%. The higher production of tetramers is probably an effect of large pore diffusion times of the primary dimer in the unground catalyst. The yield of trimers follows the same pattern as the yield of tetramers.

#### CONCLUSIONS

A high activity oligomerization catalyst based on phosphoric acid on silica has been produced by impregnation of silica spheres. A calcining temperature of 350°C is more better than calcining at 450°C or only drying at 170°C. The catalyst has a low sensitivity to water concentration in the feedstock provided it has been impregnated twice with calcination between. The activity of the catalyst produced by impregnation is higher than that of the commercial catalysts used in this study.

#### REFERENCES

1. Eglott, G., Wehnert, P.C. In Proceedings of the 3rd World Petroleum Congress, The Hague, 1951, Section IV, 201-14.
2. Engel, W.F. U.S. Patent 2 913 506.
3. Morell, J.C. U.S. Patents 3 044 964, 3 050 472, 3 050 473, 3 170 885, 3 213 035.
4. Wilshier, B.G., Smart, P. Western R., Mole T., Behrsing T. Applied Catalysis, 31 (1987), 339-359.
5. Bernard, J., Le Page, F. Ger. offen 1 954 326.
6. Corner, E.S., Lynch, C.S. U.S. Patent 3 824 149.

Table 1. Silica spheres. Properties according to manufacture.

ID	Pore Volume ml/g	Average Pore Size, Angstroms
I	1.0	300
II	1.0	600
III	1.3	600

Table 2. Silica spheres. Analytical results.

ID	Pore volume BET ml/g	Surface Area m <sup>2</sup> /g	Bulk Density g/cm <sup>3</sup>
I	0.95	79	0.43
II	0.77	62	0.40
III	0.72	60	0.36

Table 3. Conversion expressed as weight percent conversion after 20 hrs. of experiment with iso-butene. Impregnation with different acid concentrations in one step without calcination.

% P <sub>2</sub> O <sub>5</sub>	Conversion
6	20
11	22
21	17
42	6
85	9

Table 4. Selectivities

Catalyst	Time on Stream h	Weight % in Liquid			Conversion Weight %
		di-	tri-	tetra-	
Spheres III, calc 425	3	74.9	22.1	3.0	88.6
Spheres III, calc 425	23	84.0	14.9	1.1	79.6
Spheres III, calc 425	47	84.4	14.6	1.0	79.6
Spheres III, calc 350	27	73.3	22.7	4.0	97.6
Commercial unground	49	68.5	27.2	4.3	16.9
Commercial ground	49	76.5	20.7	2.8	65.4

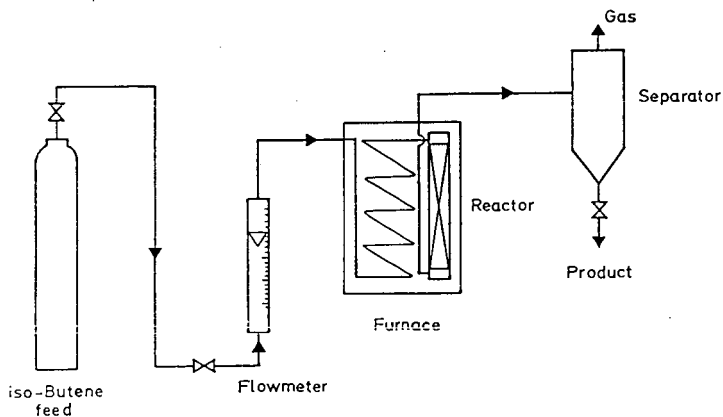


Figure 1. Simple flow diagram of reaction system.

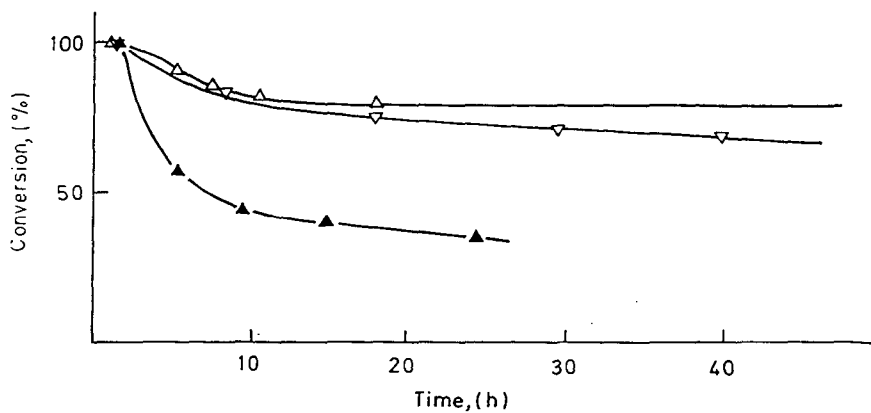


Figure 2. Conversion in weight percent of catalysts prepared with silica spheres  
 I ▲, II ▽ and III △. Calcined at 425°C and impregnated twice.

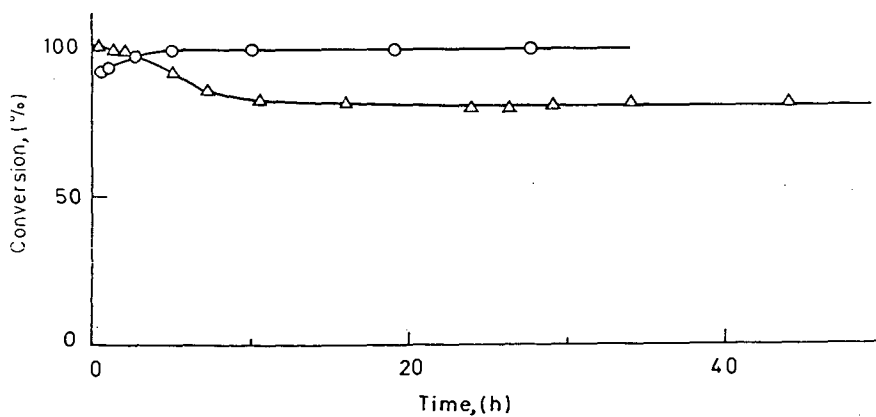


Figure 3. Conversion in weight percent of catalysts calcined at 350°C ○ and  
 425°C △. Catalysts prepared from sphere III, impregnated with  
 phosphoric acid (42%, P<sub>2</sub>O<sub>5</sub>), calcined, impregnated and dried.

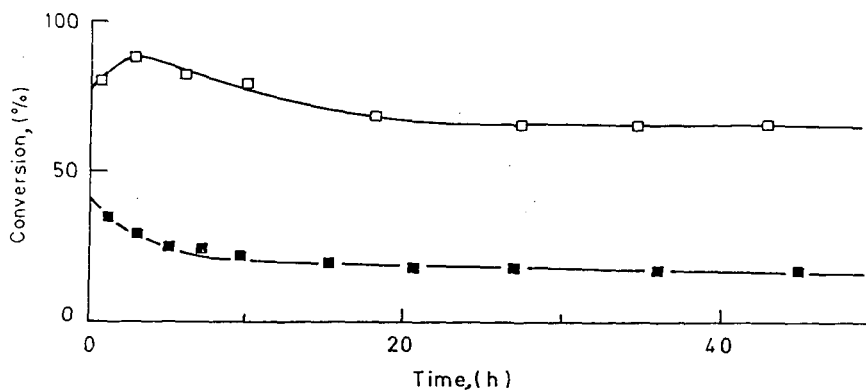


Figure 4. Conversion of commercial catalyst in weight percent. Unground ■ and ground □.